ERIODICAL
14(1)
(Nov. 62)
140

気象庁欧文海洋報告

第14巻 第1号

LIBRARY
JUN 26 1963
FISH & WILDLIFE SERVICE

THE OCEANOGRAPHICAL MAGAZINE

Vol. 14 No. 1

CONTENTS

M. HANZAWA: Studies on the inter-relationship between the sea and the atmosphere (Part 5)—Sea surface temperature anomalies in connection with the imcoming incident radiation anomalies 1

K. WATANABE: Summary of sea ice conditions off the coast of Hokkaido —Study on sea ice in the Okhotsk Sea (I) 15

K. WATANABE: Drift velocities of ice measured from air and separately computed values of their wind-induced and current-induced components— Study on sea ice in the Okhotsk Sea (II) 29

K. TERADA, H. FUTI and M. MIYAZAKI: Storm surge forecasting method and telemetering, recording, printing and indicating system of tide and other elements—so called "Call System"—in Japan 43

T. UENO: The "Component Hour" in Darwin's method for the Harmonic analysis of tides 63

Published by the Japan Meteorological Agency

November 1962

The Oceanographical Magazine
Vol. 14. No. 1, November 1962

Studies on the Inter-relationship between the Sea and the Atmosphere (Part 5)

—Sea surface temperature anomalies in connection with the incoming incident radiation anomalies—

By

Masao HANZAWA

Japan Meteorological Agency

(Received October 1, 1962)

Abstract: Since the main source of energy that maintains the temperature of the sea is the solar radiation, it is apparent that the variation of the incident solar radiation reaching to the sea surface itself is the main cause of the temperature variation of the sea surface. From this view point, characteristics of the solar radiation over the North Pacific Ocean are studied in detail. Obviously, the solar radiation affected by the existence of clouds varies considerably with space and time, and it is clarified that when under normal radiation is seen in some localities, then the temperature over the coincident area usually shows negative departures and *vice versa*. From these facts large scale negative or positive anomalies in surface water temperature over the North Pacific Ocean are explained as the results of the shortage or excess of the incident solar radiation that reaches to the sea surface. See-saw like occurrence of sea surface temperature anomalies pointed out by the present author which was seen in both sides of the North Pacific Ocean was also explained by the large scale anomalies of solar radiation over the North Pacific.

1. *Introduction*

Energy transfer between the sea and the atmosphere was stated elsewhere in the previous reports of the author. So far, it is important to know the horizontal and time variations of the total incident incoming solar radiation which reaches to the sea surface as an important index of the cause of oceanic variations. Previously, the studies of heat budget over the ocean have been based on statistical mean values of Q_s anomalies, since no synoptic values of Q_s were available.

In this treatise, however, the values of Q_s over the North Pacific Ocean are calculated for monthly basis for 5°-lat. and 5°-long. square over the period of

1911–1935. Then, the mean values over the entire period are calculated and deviations for each month are also deduced. From these values of Q_s anomalies, horizontal distribution features of these anomalies and long trends of these anomalies are considered and the simultaneous variations in oceanic conditions are studied.

2. *Theoretical considerations*

For the calculation of the total incoming radiation, MOSBY's (1936) following formula is adopted.

$$Q_s = k \cdot \overline{h} \ (g.\ cal/cm^2/min) \ . \qquad (1)$$

This is an equation with clear skies, expressed in g. cal/cm²/min. Here, k may be considered as a parameter whose values vary with the water vapor in the atmosphere. The value of k varies slightly in a narrow range and is given with a function of latitude. And $\overline{h}$ is the mean solar altitude, in degrees, during the period over which the heat is calculated. Apparently, this expression must be modified for cloudiness.

The heat exchange between the sea and atmosphere is expressed by the following equation.

$$Q_s = Q_e + Q_h + Q_b \ . \qquad (2)$$

Here, Q_s is the total incident incoming solar radiation that reaches to the sea surface, Q_e the heat used for evaporation from the sea surface, and Q_b the heat by back radiation from the sea surface, respectively. Among these quantities, actual values over the ocean have been estimated by several researchers. Estimation of the Q_e, Q_h, and Q_b was carried out by JACOBS (1942) and SVERDRUP (1937).

Previously, Q_h was deduced indirectly from sea and air temperatures by means of the so-called Bowen Ratio. Therefore, information on the actual values of Q_h has been so limited, although some measurements of actual Q_h values over the ocean with airborn instruments are being tested. Concerning the back radiation, it is very important to know the amount of water vapor content in the lower atmosphere since the water vapor plays an important role in this process. In the study of heat budget over the land area, BUDYKO (1951) has recently developed an extensive study in this field.

However, as far as the study over the oceanic area is concerned, information on the water vapor distribution in the air over the ocean is presently not available since no aerological observations taken on board of merchant ships and no wet-bulb temperature observations are usually made on board.

Corrected equation for cloudiness is given as follows:—

$$Q_s = k \cdot \overline{h}\ (1-0.71\ C) \quad (g.\ cal/cm^2/min)\ . \qquad (3)$$

Here k is a parameter, function of water vapor, $\overline{h}$ the mean solar altitude, C the cloudiness over the ocean. Here k is given in the following table.

Latitude	70–60	60–50	50–40	40–30	30–20	20–10	10–0°North
k	0.026	0.025	0.024	0.023	0.023	0.023	0.023

Latitude	0–10	10–20	20–30	30–40	40–50	50–60	60–70°South
k	0.023	0.023	0.023	0.024	0.025	0.026	0.027

In order to meet the climatological requirements of this study, the solar altitude is calculated exactly from the following equation.

$$\sin h = \sin \varphi \cdot \sin \delta + \cos \varphi \cdot \cos \delta \cdot \cos t\ . \qquad (4)$$

Here h is the altitude of the sun, φ the latitude, δ the declination of the sun, t the hour angle of the sun. And the values of $\overline{h}$ are calculated from daily means of solar altitude along with the annual variation of the solar altitude. Daily means are calculated from the solar altitude values of 06h to 18h, and the annual values are deduced taking the value of 15th day of that month is assumed to be a mean of the said month.

Using this formula, monthly mean incoming radiation values for each month over the North Pacific Ocean are calculated. As for the basic marine meteorological data, "Marine Meteorological Data over the North Pacific" issued by the Imperial Kobe Marine Observatory are adopted.

Coverage of calculation was for the North Pacific Ocean in space and the period of 1911–1935 in time. Mean monthly value for the 1911–1935 period were obtained, along with the anomalies for each month based on the means of 1911 to 1935.

The results of calculation show that the incoming radiation value are somewhat larger than those obtained previously by MOSBY and others. However, recent estimation by ANDERSEN (1959) also affirms that MOSBY's values were underestimated to some extent. LAEVASTU's recent study (1960) based on the actual pyreheliometer observations obtained on board the U. S. S. *Rehoboth* also coincide with our estimation.

3. Features of the incoming radiation over the North Pacific Ocean

All calculated incoming radiation values are plotted on charts in the grid of 5°-lat. and 5°-long. square. Monthly mean charts are shown in Fig. 1-12. Glancing the mean charts for the period of 1911-1935, represented separately for each month, we noticed the following characteristic points.

(1) Theoretically speaking, all isolines of the incident incoming radiation should be paralleled with latitude lines since solar radiation that reaches to the sea surface would be determined only by the altitude of the sun if no affecting meteorological influences are existed. However, actual isolines show somewhat different fashion because of existence of clouds and other various causes.

(2) Isolines generally parallel with latitude lines for the area between 155°E-145°W.

(3) However, in the southwestern Pacific, the isolines show a little bit complicated fashion and do not parallel with the latitude lines.

(4) In the southeastern Pacific, the isolines show up complicated fashion especially between Hawaii and Baja California.

Causes of these irregularities of equi-radiation lines are not clarified yet but it seems plausible that the variation of local meteorological phenomena such as the generation of typhoons, disturbances caused by easterly waves etc. may contribute to the occurrence of these irregularities.

4. Time variations of radiation in connection with oceanic variations

As is shown everywhere in the previous reports of the author, HANZAWA (1952, 1956, 1957, 1958a, and 1958b), it is apparent that when a peculiar atmospheric pressure deviation anomaly pattern appears over the entire North Pacific Ocean, a particular distribution of sea surface temperature anomaly usually takes place.

From the long-term mean charts of the incoming incident solar radiation over the North Pacific Ocean (Fig. 1-12), we calculated deviations of 5°-lat. -long. squares for every month of 1911-1935. These deviation charts are not reproduced here but from these charts we could say there is a systematic fashion in deviation charts. These are as follows:—

(a) It is plausible that a pattern of deviation chart seems to have conservative property, namely, when a particular pattern once appears, the similar pattern seems to persist for considerable period on a series of monthly

mean charts.

(b) Area of negative or positive anomalies does not show diverged fashion but shows rather coagulated fashion. Namely, a couple of blocks of positive or negative area are seen in deviation charts.

From these facts, we may say that there is a kind of persistency in solar radiation even on the monthly mean basis charts. In order to see the influence of solar radiation over the oceanic conditions, the July charts of 1926, 1933 and 1934 are reproduced (Fig. 13-15). The cases are considered as of peculiar years. Namely, in these years, meteorological, consequently oceanographic conditions over the North Pacific Ocean are very peculiar as are concluded from the anomalies of sea surface temperatures and the so-called see-saw like (one coast is high and the other coast is low in the North Pacific Ocean) appearance of surface temperatures were observed. Deviation charts of radiation intensities of these years also show the similar fashion and from this we can deduce that solar radiation is, basically, closely connected with atmospheric deviation.

Through the course of 1926, the sea surface temperatures along the coast of North America showed very high positive anomalies. In accordance with this state, the solar radiation showed positive anomalies. Along the belt of 30°–40°N, solar radiation anomalies were high having the value of +0.41 g. cal/cm^2/min up to about 160°W.

On the contrary, radiation anomaly in the western side of the Pacific shows negative values up to −0.28 g. cal/cm^2/min especially in the southern seas of Japan.

The cases of the summer of 1933, when a very vivid see-saw like appearance of sea surface temperature anomalies were observed having positive values in the western side and negative values in the eastern side, and the radiation anomaly chart also shows consequent fashion. In the previous report of the present author and T. INOUE (HANZAWA, M. and T. INOUE, 1952), the case of July 1933 sea surface temperature was analysed in detail.

Comparing the sea surface temperature and solar radiation anomaly charts of July 1933, again we notice the strong negative anomaly of solar radiation along the American coast and positive anomalies in the central part of the North Pacific. The similar but reversal condition is found for the case of July 1934.

Judging from the above analysis, we may conclude that excess or deficit of solar radiation over a considerable sea area will bring about warming or cooling

of the water *in situ*. In addition to the above effect, prevalence of above or under normal condition of the North Pacific Anticyclone will produce more supply of warm water from the southern side or cold water from the northern side.

Acknowledgements: The author wishes to express his gratitude to Prof. Yoshio KATO, Geophysical Institute, Tohoku University, Prof. Giichi YAMAMOTO, Geophysical Institute, Tohoku University and to Dr. Kazuhiko TERADA, Japan Meteorological Agency for their kind advice and suggestions.

References

ANDERSON, E. R. (1959): Energy-budget studies. Water loss investigatioes: Lake Hefner Studies. *U. S. Geol. Survey, Prof. Pap.* 269: 71–119.

Гудьико, М. И. (1956): Тепловой ъаланс земной поверхности. Гидрометеорологическое Издатедьство. Ленинград. 254.

HANZAWA, M. and T. INOUE (1952): Relation between oceanic and atmospheric state in the North Pacific Ocean for the year of bad and good rice crop (In Japanese). *Oceanogr. Rep. Cent. Met. Obs.*, **2** (3), 65–70.

HANZAWA, M. (1956): Preliminary report on a close relationship between surface temperatures at the two separated stations, Papa and Tango. *Oceanogr. Mag.*, **8** (2), 157–160.

HANZAWA, M. (1957): Studies on the inter-relationship between the sea and the atmosphere (Part 2). *Oceanogr. Mag.*, **9** (1), 87–93.

HANZAWA, M. (1958): Studies on the inter-relationship between the sea and the atmosphere (Part 3). *Oceanogr. Mag.*, **10** (1), 91–96.

HANZAWA, M. (1958): Studies on the inter-relationship between the sea and the atmosphere (Part 4). *Oceanogr. Mag.*, **10** (2), 215–226.

JACOBS, W. (1942): On the energy exchange between sea and atmosphere. *Journ. Mar. Res.*, 5, 37–66.

Kobe Marine Observatory: The mean atmospheric pressure, cloudiness, air temperature of the North Pacific Ocean. Series.

LAEVASTU, T. (1960); Factors affecting the temperature of the surface layer of the sea. *Societas Scientiarum Fennica, Comm. Phys.-Math.* XXV, 1–136.

MOSBY, H. (1936): Verdunstung und Strahlung auf dem Meere. *Ann. Hydrogr.*, Berlin, 64, 281–286.

SVERDRUP, H. U. (1937): On the evaporation from the oceans. *Journ. Mar. Res.*, **1** (1), 3–14.

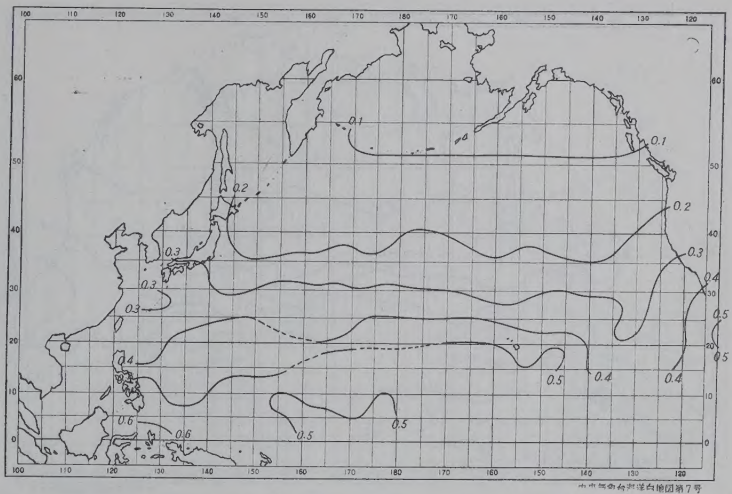

Fig. 1. Monthly mean incident solar radiation: January (Unit: g. cal/cm²/min)

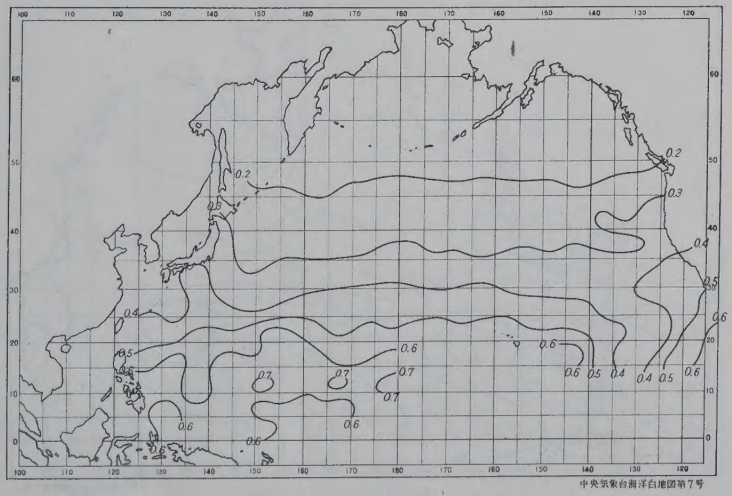

Fig. 2. Monthly mean incident solar radiation: February (Unit: g. cal/cm²/min)

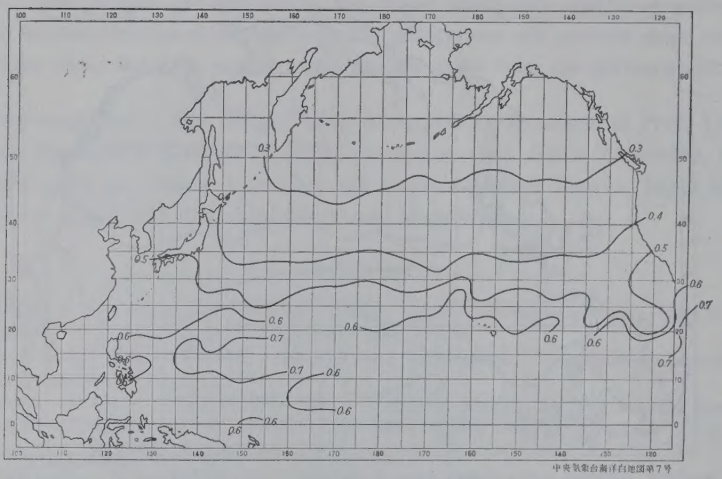

Fig. 3. Monthly mean incident solar radiation: March (Unit: g. cal/cm²/min)

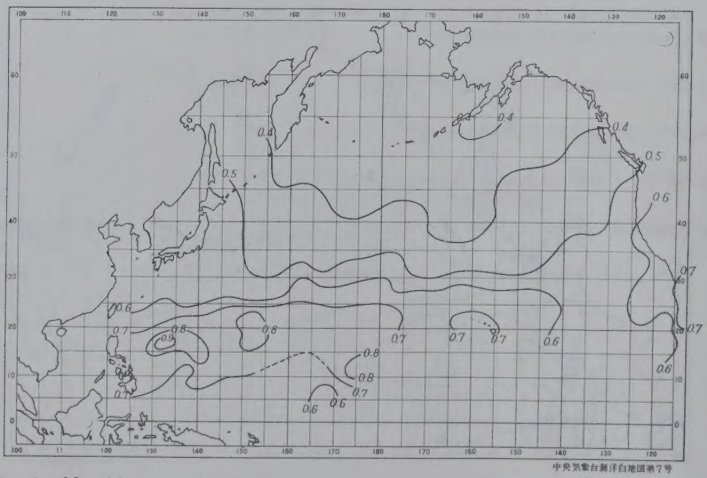

Fig. 4. Monthly mean incident solar radiation: April (Unit: g. cal/cm²/min)

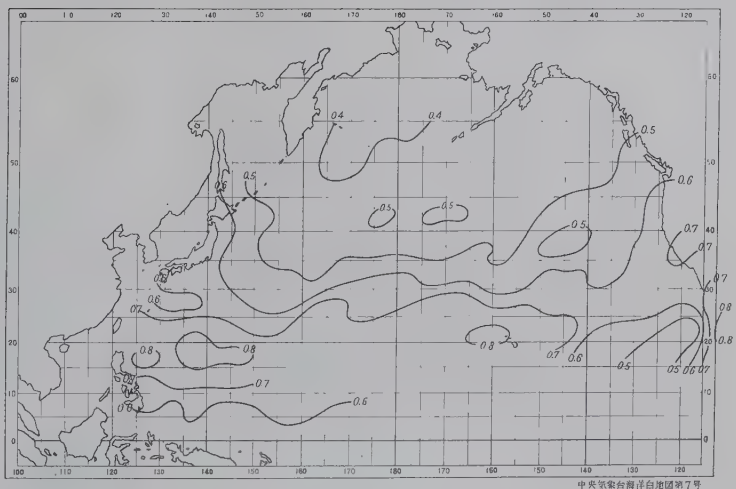

Fig. 5. Monthly mean incident solar radiation: May (Unit: g. cal/cm²/min)

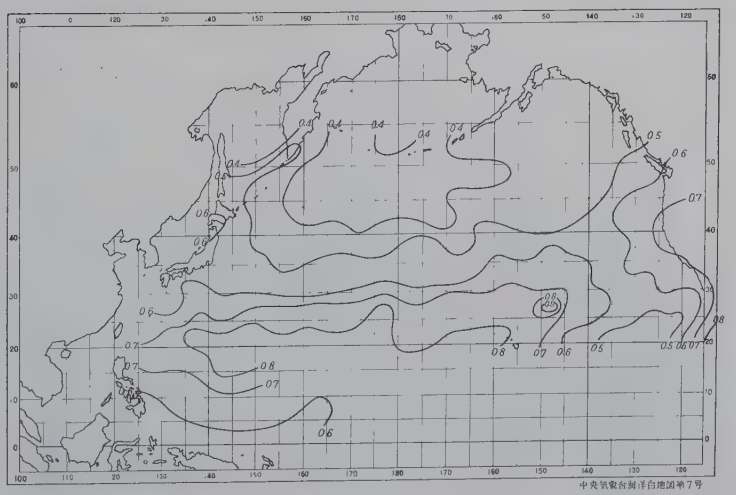

Fig. 6. Monthly mean incident solar radiation: June (Unit: g. cal/cm²/min)

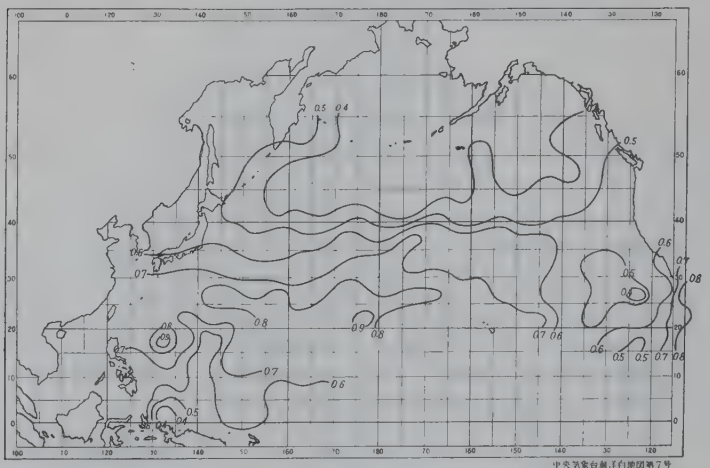

Fig. 7. Monthly mean incident solar radiation: July (Unit: g. cal/cm^2/min)

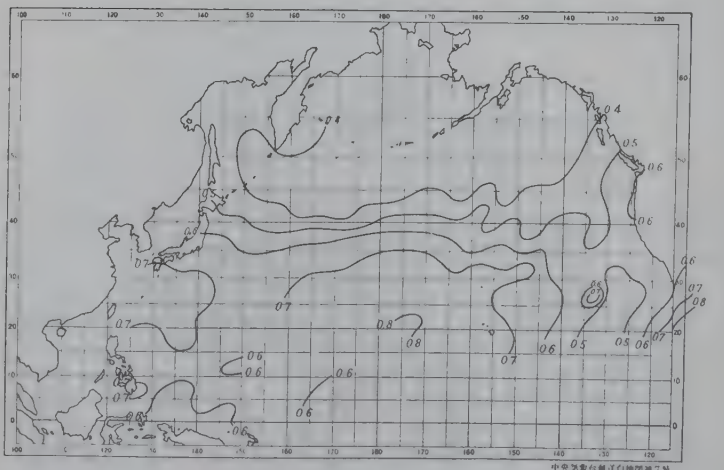

Fig. 8. Monthly mean incident solar radiation: August (Unit: g. cal/cm^2/min)

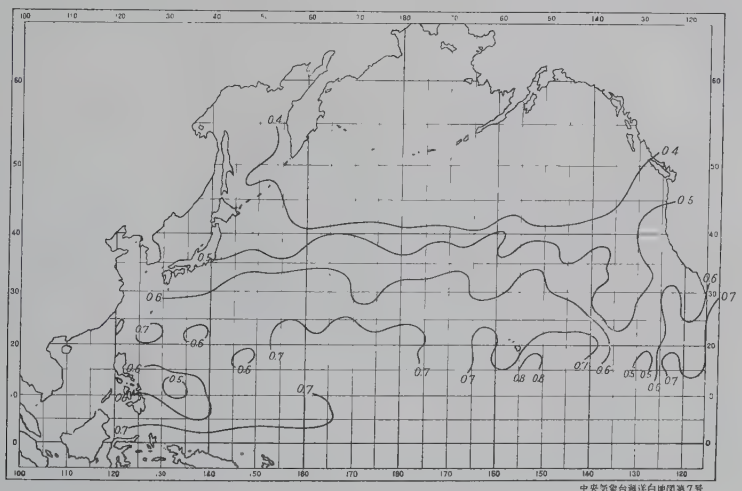

Fig. 9. Monthly mean incident solar radiation: September (Unit: g. cal/cm²/min)

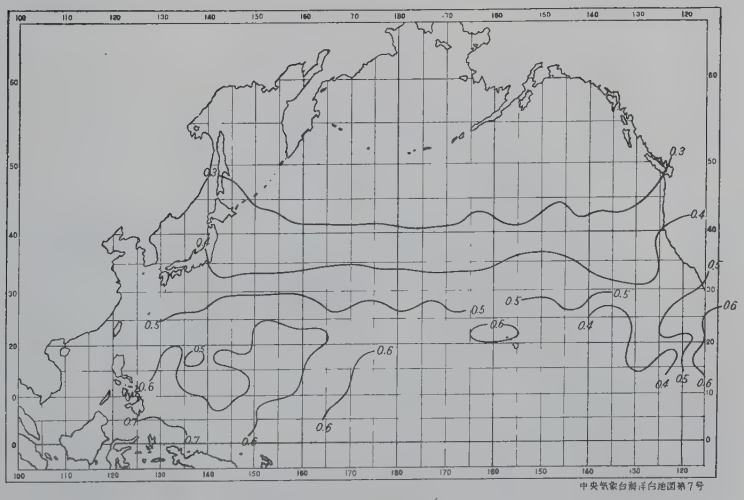

Fig. 10. Monthly mean incident solar radiation: October (Unit: g. cal/cm²/min)

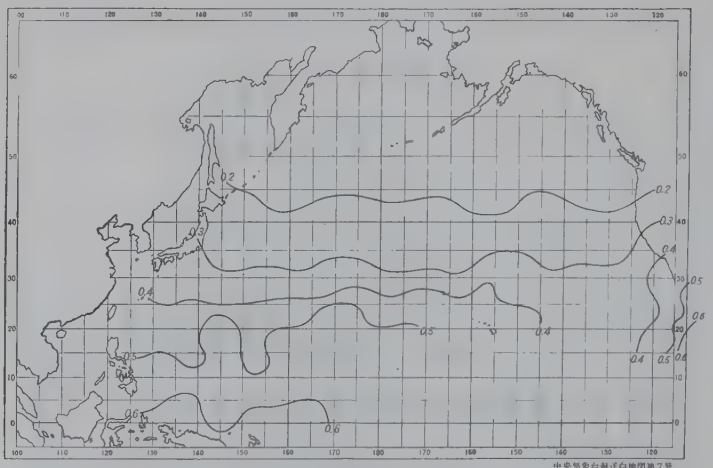

Fig. 11. Monthly mean incident solar radiation: November (Unit: g. cal/cm²/min)

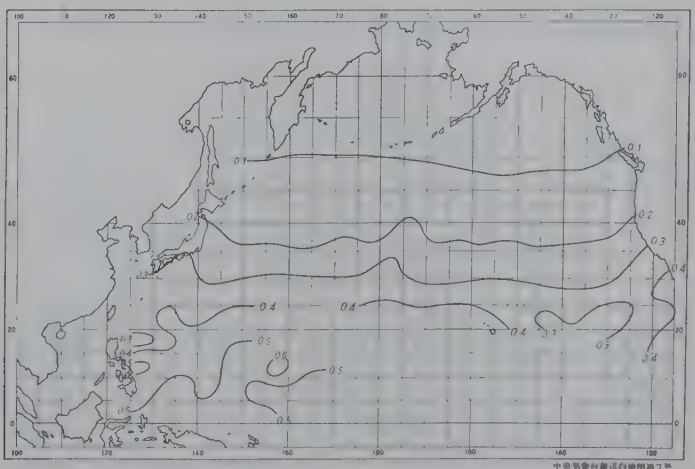

Fig. 12. Monthly mean incident solar radiation: December (Unit: g. cal/cm²/mid)

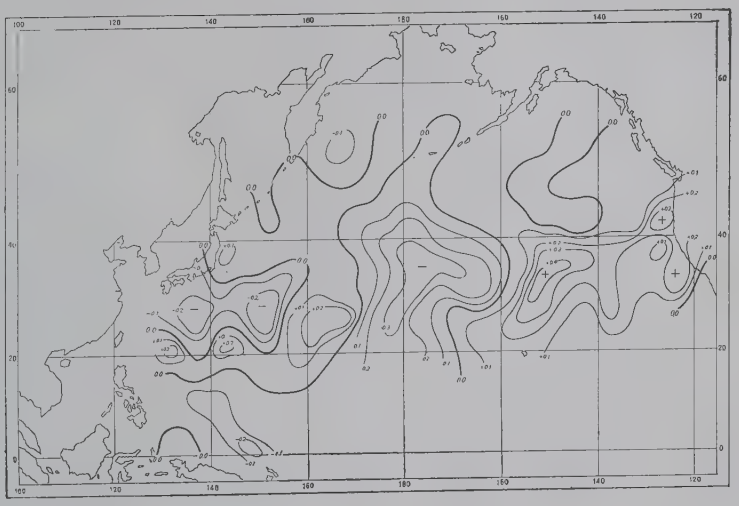

Fig. 13. Anomalies of the incident solar radiation: July 1926. (Unit: g. cal/cm²/min)

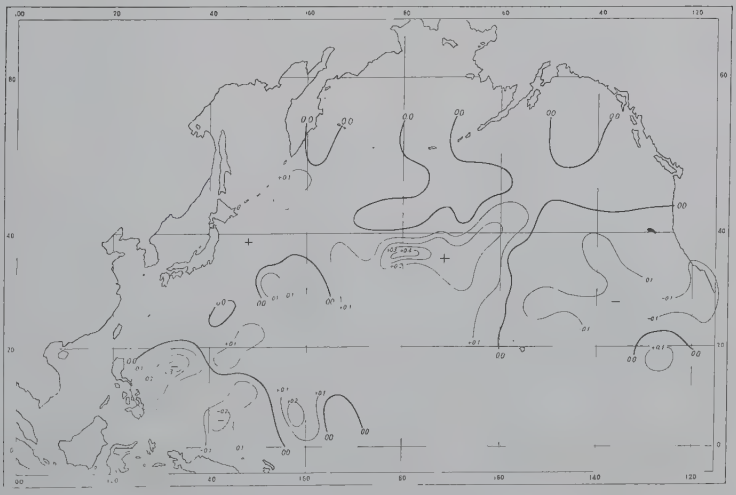

Fig. 14. Anomalies of the incident solar radiation: July 1933. (Unit: g. cal/cm²/min)

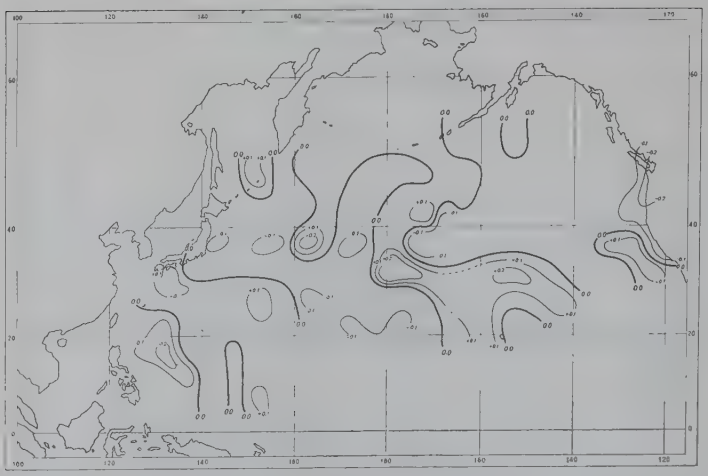

Fig. 15. Anomalies of the incident solar radiation: July 1934. (Unit: g. cal/cm²/min)

The Oceanographical Magazine
Vol. 14. No. 1, November 1962

Summary of Sea Ice Conditions off the Coast of Hokkaido

—Study on Sea Ice in the Okhotsk Sea (I)—

By

Kantaro WATANABE

(Received October 15, 1962)

Abstract: In the present paper, the first one in a series of the author's studies on sea ice in the Okhotsk Sea, are summarized the sea ice phenomena off the coast of Hokkaido, being based on the data collected in the aerial sea ice reconnaissance since 1957. The processes of appearing off the coast and extending there and retreating from there of drift-ice are glanced in referring to the differences of ice conditions in each winter. As a noticeable phenomenon observed in the drift-ice there, are presented the characteristic patterns of ice covers arranging in numerous streams along the ocean current. Besides, the drifting route of ice is discussed by detail ice charts rectified from aerial photographs.

1. Introduction

An enormous amount of drift-ice together with newly formed sea ice blocks partly or entirely the Okhotsk coast of Hokkaido during winter. It affects seriously to the life and industries there, perfectly stopping the fishery and its correlated industries, and occasionally giving a large damage on the agriculture (SAWADA, 1956).

The first regular observations of sea ice in Japan were started at several weather stations and lighthouses located along the Okhotsk coast of Hokkaido in 1892, and eight shore weather stations and several lighthouses around Hokkaido are continuing them at present. But their observable sights are confined so close to the shore that the available data on sea ice are very incomplete for studing ice conditions on the broad sea surface or for making ice prognoses.

The aerial sea ice reconnaissance had been made in the southwestern region of the Okhotsk Sea by the aircrafts of the Central Meteorological Observatory (the former name of the Japan Meteorological Agency) since 1935 and lasted to 1944. Though the large part of its data were unfortunately burnt away by the Second World War, the remaining data were published as sea ice charts from the Hakodate Marine Observatory (1955). In the almost same period sea ice reconnaissances in the Okhotsk Sea had been made also by the aircrafts and ships

belonged to the former Japanese Navy, which data were summarized by S. KURASHINA (1954, 1958).

After a somewhat long time passed in lacking ice data from air since the last of the War, the aerial sea ice reconnaissance that is more systematic and precise than the former ones has been renewed by the Sapporo District Meteorological Observatory and the Hakodate Marine Observatory, both are the branches of the J. M. A., in cooperation with the Japan Defence Agency since 1957. In this operation an aircraft of three types, jet aircraft T-33A, Neptune P2V and Cessna L-19, has flung along the coast of Hokkaido nearly twice a period of 10-days during from the last of December until the end of the following April in every winter. The sea and sea ice have been taken in oblique photographs in

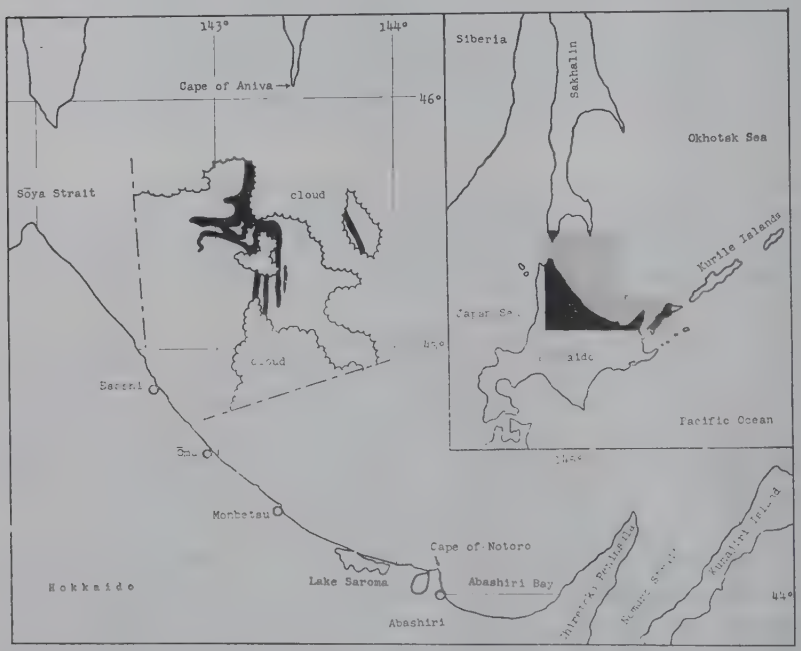

Fig. 1. Ice chart on Jan. 7, 1959. The blackened area represents an ice cover, an accumulation of brash-ices and ice-cakes. This and the other ice charts in the present paper have been made by a method of aerial photogrammetry (WATANABE, 1961).

each flight and they have been rectified in an ice chart by the method of photogrammetry developed by the author (WATANABE, 1961). The ice charts made in the operation have been or will be presented by the author and others elsewhere (J. M. A., 1958, 1961, 1962 and 1963: H. M. O., 1959).

According to the operation since 1957, our knowledges on sea ice off Hokkaido have become extremely rich and are now growing richer and richer. The secrets of drift-ice there, the processes of its appearing and extending or retreating have been considerablly revealed. The drifting route and velocities of ice have been first grasped and their dependence to the ocean current has been reasonablly assumed. In the consequence of such growing of our knowledges, have been able to be estimated the mechanism of sudden reinforcement of the East Sakhalin Current in early winter, to which the sea ice phenomena off Hokkaido is greatly responsible, and the origin of drift-ice appearing off Hokkaido in every winter. Furthermore, some distributions of freezing area in the whole Okhotsk Sea have been estimated for early ice season by decreasing temperature gradients of surface water, and mean ice limits in the sea were made for each month from available data on ice covers hitherto obtained in Japan. These items are treated in this paper and the serial papers on the present thesis.

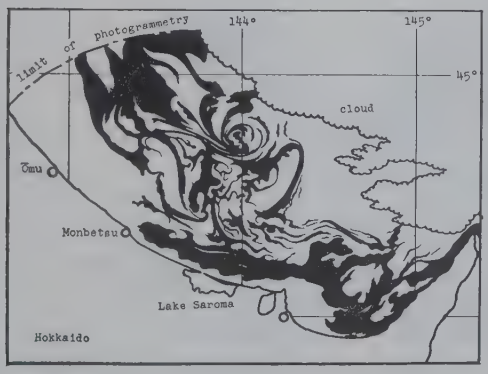

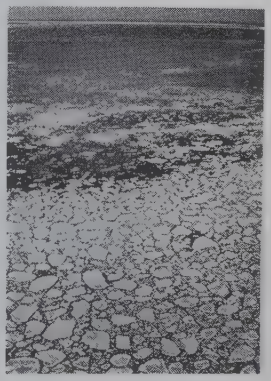

Fig. 2. (left). Ice chart on Jan. 28, 1959. From these numerous ice streams and an icy eddy it should be noticed that the existence of an ocean current there and also its fine structure are reasonably suggested.

Fig. 3. (right). Aerial view of drifting ice-floes in early ice season (from an altitude of about 100 m, in the Abashiri Bay, on Jan. 24, 1959).

2. First appearance of drift-ice off the coast of Hokkaido

It is usually at the beginning of January that the first drift-ice appears off the Okhotsk coast of Hokkaido in every winter. An accumulation of drifting small ice-floes, ice-cakes and brash-ices in a few belts or many streams comes from the east offing of the Cape of Aniva, one of the southern tips of Sakhalin, and runs towards the coast of Hokkaido in that period as illustrated in Fig. 1. Most of floes of such first appearing drift-ice are about 30 cm to 50 cm in thickness, not about 20 cm or thinner. This fact in ice thickness gave the author to estimate their origin to be in the east offing of northern Sakhalin, and the average speed of their drift at 0.6 kt or faster. The method of the estimation will be presented in one of the later papers in this series (WATANABE, 1963b).

The drift-ice usually reaches the coast from about Ōmu to Abashiri at the middle of January, then gradually extends towards the tip of the Shiretoko Peninsula and farther east as shown in Fig. 2. Fig. 3 is an aerial view of such drifting ice-floes in that period which were estimated at about 0.5 m in thickness.

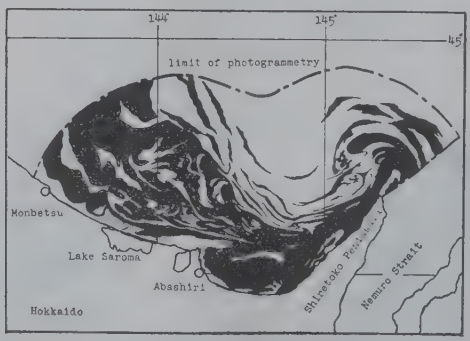

Fig. 4. Ice chart on Feb. 12, 1959. This arrangement of parallel ice streams shows the drifting route of ice along the ocean current, an end flow of the East Sakhalin Current.

In almost every winter the drift-ice rapidly grows in its extent and size of each floe during the last 10-day period of January.

3. Characteristic pattern of ice covers in light ice period

As illustrated in the ice charts of Figs. 2 and 4 and seen in the photograph

of Fig. 5, ice covers in the advance period of rather light ice winter are usually of very complex pattern of numerous belts and streams sometimes being associated with icy eddies, suggesting that the drift-ice is carried mainly by the ocean current, and also that the ocean current consists of numerous vertically converging or diverging lines of horizontally flowing water on which converging lines

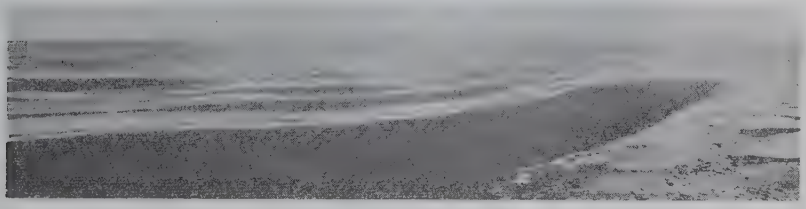

Fig. 5. Aerial view of the ice streams charted in Fig. 4 (from an altitude of 6,000 ft above the Cape of Notoro, on Feb. 12, 1959). The ice current directs eastward from the northwest. Each stream consists of mainly ice-cakes and small ice-floes.

ice-floes aggregate in streams when the closeness of ice is low. Such characteristic arrangements of ice streams were observed always in the advance period until the middle of February in 1957 and 1959, and the end of February in 1958

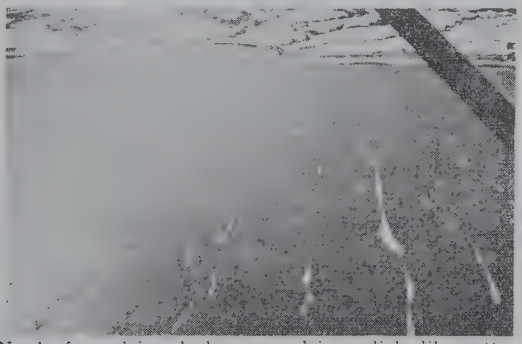

Fig. 6. Newly formed ice slush arranged in a slicks-like pattern (from about 150 m altitude, near the shore of the Abashiri Bay, on Jan. 29, 1959). These lines of ice slush parallel to the wind direction seem to occur upon wind-induced linear zones of convergence of surface water as the natural slicks on the ocean reported by Robert S. DIETZ and his cooperator (1950) and Alfred H. WOODCOCK (1950).

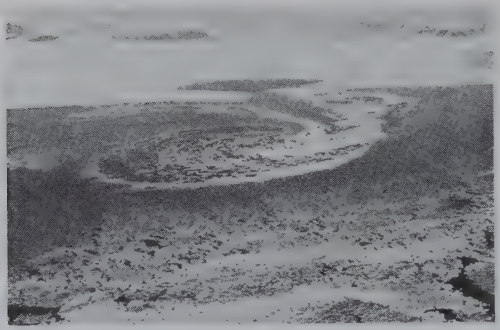

Fig. 7. Icy eddy appearing at the mouth of Lake Saroma (from an altitude of 1,000 ft, on Feb. 12, 1959). This eddy deflected east (left hand in the picture) from the centre of the mouth shows the existence of an eastward current along the coast.

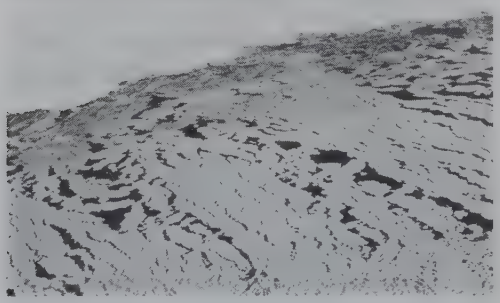

Fig. 8. Young ice formed near an edge of drift-ice cover (from an altitude of 3,000 ft off the coast near Lake Saroma, on Feb. 12, 1959). The bright area in the background is drifting winter-ice and the grey one in the foreground is young ice with numerous cracks being formed by the action of wind and current.

as shown in many ice charts prensented on the above referred reports of this operation.

In open water by or between ice streams, or in cracks, leads and polynias in ice fields, there occur the formation and development of new ice of all types from muddy ice slush to flat young ice, then to winter-ice, as seen in the photographs of Figs. 6, 7 and 8, in spite of the location at such low lattitude as

44° N or lower. This is mainly responsible to the well-cooled low saline water coming with the drift-ice from the northwestern area of the sea along the East Sakhalin Current intensified in winter season, where a strong stratification exists in surface layer because of the small density of its water (WATANABE, 1959, 1963c).

4. Reinforcement of ice conditions in heavy ice winters

In contrast to such rather light ice conditions in early ice seasons of 1957,

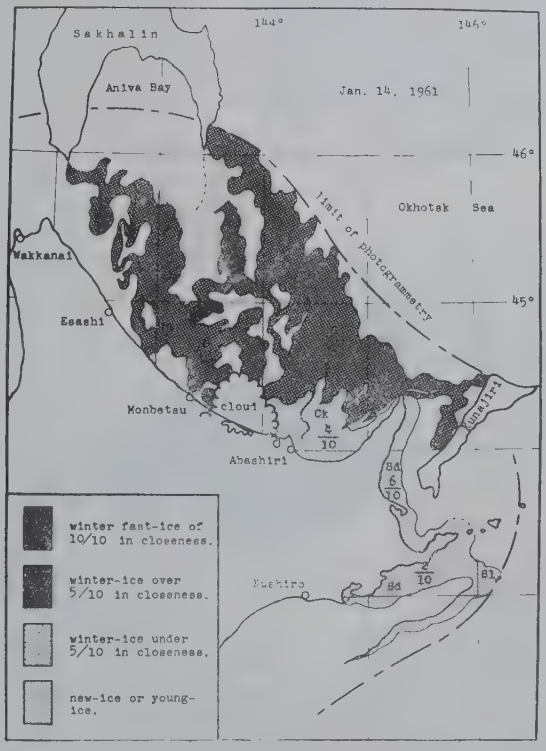

Fig. 9. Ice chart on Jan. 14, 1961. In the winter of 1961, the heaviest ice winter since the aerial sea ice reconnaissance started in 1957, the ice cover suddenly extended in the second week of January, then the ice conditions became heavier at the end of the month than the maximum ice conditions in the past four winters.

1958 and 1959, very heavy states of ice occurred in the same period in 1960 and violently in 1961. Drifting few ice streams were early observed from an aircraft 20–30 nautical miles off the coast from Esashi to Monbetsu on Dec. 24, 1960. Though at the beginning of January in 1961 the ice conditions did not differ so much from those in the same period of the past four years, a rapid reinforcement of ice extent and amount of ice occurred at the second week of the month. Fig. 9 is the ice chart on Jan. 14, 1961 which shows ice covers of winter-ice widely extending off the coast in such early ice season. The ice conditions became heavier and heavier during the last half January in both 1960 and 1961, then the coast from the Cape of Sōya to the tip of the Nemuro Peninsula was almost perfectly blocked by predominatingly developed winter-ice of all sizes

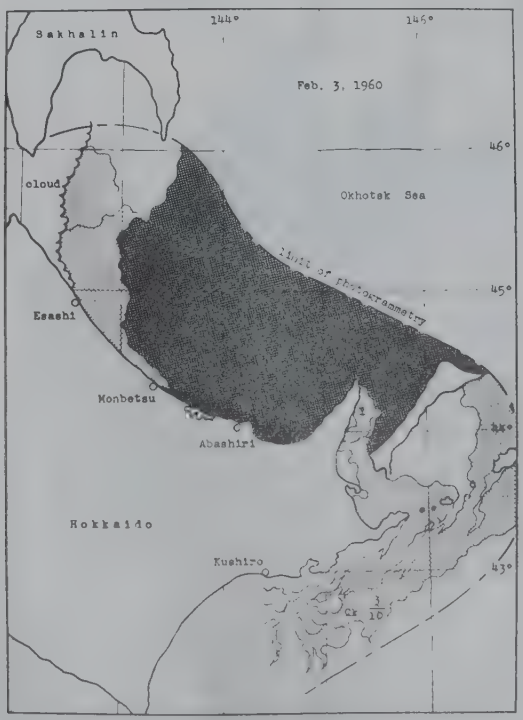

Fig. 10. Ice chart on Feb. 3, 1960.

from brash ice to vast ice-floe with hummocks of 2-3 m high above sea level here and there. Fig. 10 is an ice chart on Fig. 3, 1960, in such conditions and Fig. 11 is a photograph of the Abashiri Bay perfectly blocked by very close pack-ice in the same day. Thus, the maximum intensity of ice conditions began at the beginning of February in 1960 and at the end of January in 1961, and it lasted to the end of February in 1960 and to about the end of March in 1961. But it occurred in March in 1957 and rather weakly in the period from February until the beginning of March in 1958 and very weakly only in February in 1959.

Fig. 11. Very close pack-ice perfectly blocking the Abashiri Bay (on Feb. 3, 1960).

5. Drifting route of ice in advance period

From the above description the drifting route of ice may be easily grasped for the area off Hokkaido in advance period. That is, the drift-ice coming southward from the east offing of southern Sakhalin runs usually along the coast of Hokkaido towards the tip of the Shiretoko Peninsula, then flows out to the area north of the southern Kurile Islands or into the Nemuro Strait as illustrated in Fig. 12 and 13. Such drifting route of ice has been more vividly shown in Fig. 21 at page 103 in the author's former paper (WATANABE, 1961) and Fig. 8 at page 8 in one of the reports of this operation (J. M. A., 1961).

Drift velocities of ice along such route were measured in three cases by the author by means of inspecting displacements of ice masses or icy eddies in the ice charts on successive days, namely, at 0.4—0.8 kt of scattered ice streams off the Abashiri Bay at the middle of February in 1957, and 0.3—0.4 kt of icy eddies off Lake Saroma and the Cape of Notoro at the begining of February in 1959, and 0.3—1.0 kt of ice streams off the coast from Monbetsu to the tip of the Shiretoko Peninsula at the middle of the same month (WATANABE, 1963 a).

Now, in heavy ice period a small part of the Okhotsk drift-ice flows out through the Sōya Strait into the Japan Sea, but it rapidly melts away there by the action of warmer and higher saline water from the Tsushima Current. And also some part of the drift-ice passes through the Nemuro Strait and the chan-

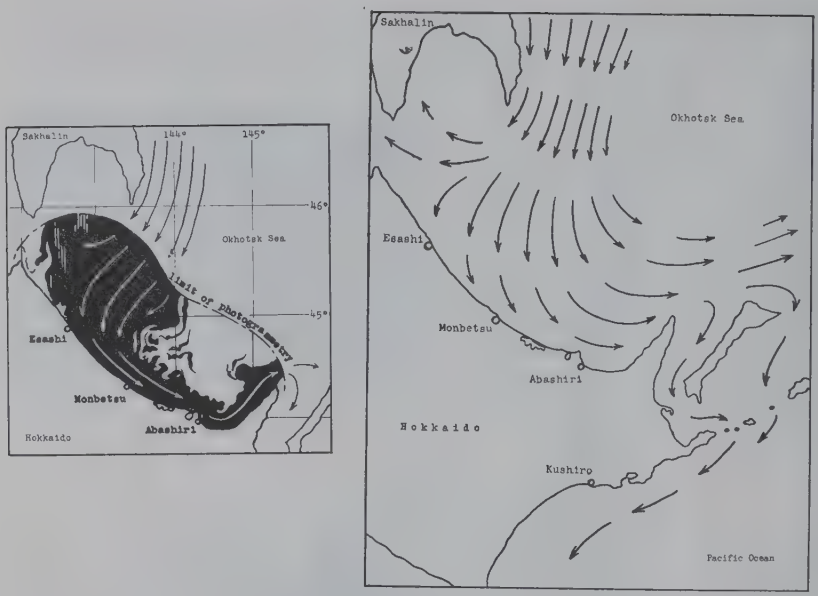

Fig. 12. (left). Drifting route of ice in light ice period with the ice chart on Feb. 19, 1958, superimposed.

Fig. 13. (right). Schematic representation of the drifting route of ice in heavy ice period as in 1960 and 1961.

nels among the southern Kurile Islands into Pacific Ocean, then flows southwestward along the Oyashio Current off the southeast coast of Hokkaido as shown in Figs. 10 and 13. Such outflows of the Okhotsk drift-ice occur only in heavy ice period as the middle of March in 1957, February in 1960, and the period from the end of January to the beginning of April in 1961. Neverthless, the major part of the Okhotsk drift-ice usualy extends to the area off the northern Kurile Islands and seems to disperse and melt away there.

Since the ice current off the Okhotsk coast of Hokkaido directs southeast- or east wards towards the Shiretoko Peninsula and the prevailing winds during winter are northwesterly, a strong ice pressure is applied southeastward to ice fields in the Abashiri Bay and its vicinity, forming very close pack-ice fields there as seen in an ice chart of Fig. 14. Especially in the heavy ice period as in 1960 and

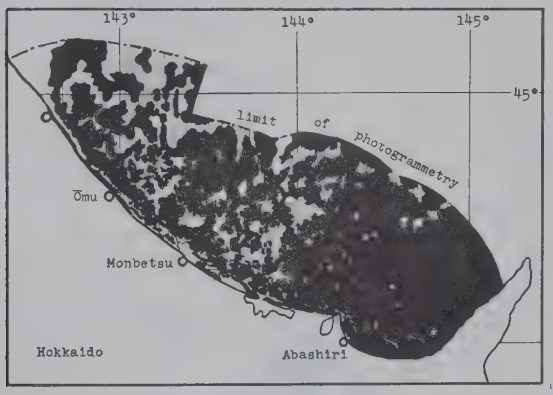

Fig. 14. Ice chart on Mar. 7, 1957. This pattern of ice cover in which the closeness of ice is highest near the coast of the Shiretoko Peninsula, shows that a strong ice pressure is applied southeastward to each ice field by the combined action of the northwesterly winds and the ocean current.

1961, the bay was completely blocked by heavy ice field (Fig. 10) and numerous pressure ices of about 2–3 m high above sea level were observed in the area near the Shiretoko Peninsula as seen in Fig. 15.

The origin of such drift-ice flowing along the coast of Hokkaido has been reasonably estimated by the author to be mainly in the area off northern Sakhalin or farther north (WATANABE, 1963 b).

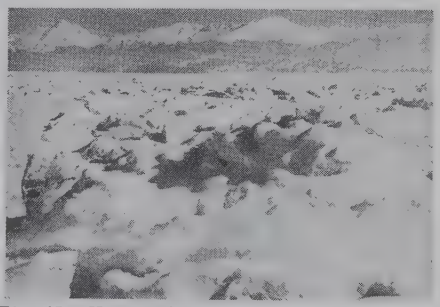

Fig. 15. Hummocks formed by ice pressure acting shoreward in the Abashiri Bay (on Feb. 6, 1961). The back ground is a part of the mountain range in the Shiretoko Peninsula.

6. *Retreat of ice covers in April*

In winter season, the southward flow of drift-ices from the northern area of the Okhotsk Sea along the East Sakhalin Current are accelerated by the northwesterly winds, thus the ice conditions off the coast of Hokkaido show their maximum intensity in midwinter as mentioned above. But in early spring the

edge of ice cover off the coast begings with the offshore retreat as monsoon-like northwesterly winds weaken. Fig. 16 is an example of ice charts in such retreating stage. Usually the ice edge continues to move eastward during April, as presented in T. SAWADA's report (1958) on the daily movement of pack-ice edge

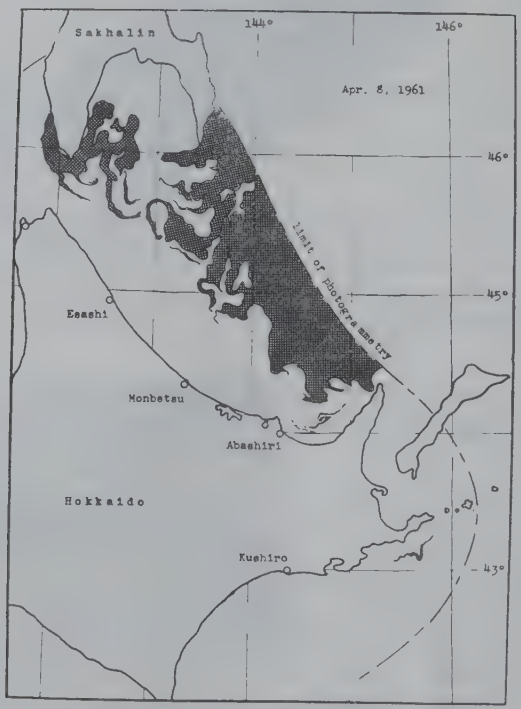

Fig. 16. Ice chart on April 8, 1961, an example of ice cover in the retreating stage.

in the southwestern area of the Okhotsk Sea in thawing period of 1956. Then, the ice season is over in the area about 100 nautical miles off the coast of Hokkaido by the end of April, though the inshore fishery is sometimes interrupted by occasional appearance of some scattered masses of ice-floes in midspring as at the end of May in 1944.

Acknowledgment: The author wishes to thank the members in the flight crews of the North Army of the Ground Self-Defence Force, the Hachinohe Combat Wing of the Maritime Self-Defence Force, and the 2nd Combat Wing of the Air Self-Defence Force for their cooperations to our aerial sea ice reconnaissance since 1957, and thank the members of the Sapporo District Meteorological Observatory, the Abashiri Local Meteorological Observatory, and the Hakodate Marine Observatory, who were engaged in the aerial observations of sea ice or the rectifications of numerous aerial photographs with the author during these five years. The author wishes also to express his sincere thanks to Dr. Kazuhiko TERADA of the Japan Meteorological Agency, Mr. Tamotsu YAMAOKA of the Sapporo District Meteorological Observatory and Mr. Zen'ichi YASUI of the Hakodate Marine Observatory for their constant encouragement throughout this work.

References

DIETZ, R. S., E. C. LAFOND (1950): Natural slicks on the ocean. *Jour. Mar. Res.*, **9** (2), 69–76.

Hakodate Marine Observatory (1955): Sea ice charts (in Japanese).

—— (1958): Aerial observation of sea-ice in the southwestern region of the Okhotsk Sea (1958) (in Japanese). *Marine Meteor. Rep. of the H. M. O.*, **2** (2), 15–34.

Japan Meteorological Agency (1958): Sea ice report of Japan (in Japanese). *Memoirs of the J. M. A.*, **40** (1).

—— (1961): Sea ice observation along the Okhotsk coast of Hokkaido from January to April 1959 (in Japanese). *Technical Rep. of the J. M. A.*, 10.

—— (1962): Sea ice observation along the Okhotsk coast of Hokkaido from January to April 1960 (in Japanese). ibid., 19.

—— (1963): Sea ice observation along the Okhotsk coast of Hokkaido from December to April 1961 (in Japanese). ibid. (in preparing to press).

KURASHINA, S. (1954): Sea ice in the Okhotsk Sea (in Japanese). *Hydro. Bull.*, 40, 1–12.

—— (1958): On sea ice in the adjacent sea of Japan (mainly on the relation between navigation and sea ice) (in Japanese). ibid., 56, 23–31.

SAWADA, T. (1956): On the damages brought about by sea-ice in 1956 (I) (in Japanese). Snow and Ice, **18** (3), 12–22.

—— (1958): On the daily ice-edge displacements of the pack-ice area covered on entire southern Okhotsk Sea in thawing time, 1956 (in Japanese). *Memoirs of the J. M. A.*, **40** (1), 117–124.

WATANABE, K. (1959): Sudden change of sea conditions preceding to the appearance of drift-ice off the Okhotsk coast of Hokkaido (in Japanese). *Tenki* (published monthly by the Meteor. Soc. of Japan), **6** (6), 190–195.

—— (1961): On the theory and technique of an easy method of wide range photogrammetry for the observations of sea ice distribution. *Oceanogr. Mag.*, **12** (2), 77–121.

—— (1963 a): Drift velocities of ice measured from air and separately computed values

of their wind-induced and current-induced components —Study on sea ice in the Okhotsk Sea (II)—. ibid., **14** (1).

—— (1963 b): On an estimation for the origin and the drifting rate of pack-ice appearing off the coast of Hokkaido —Study on sea ice in the Okhotsk Sea (III)—. ibid. **14** (2)

—— (1963 c): On the sudden reinforcement of the East Sakhalin Current preceding to the sea ice season off the coast of Hokkaido —Study on sea ice in the Okhotsk Sea (IV)—. ibid.

WOODCOCK, A. H. (1950): Subsurface pelagic Sargassum. *Jour. Mar. Res.*, **9** (2), 77–92.

The Oceanographical Magazine
Vol. 14. No. 1 November, 1962

Drift Velocities of Ice measured from Air and Separately Computed Values of Their Wind-induced and Current-induced Components

—Study on Sea Ice in the Okhotsk Sea (II)—

By

Kantaro WATANABE

Hakodate Marine Observatory

(Received October 29, 1962)

Abstract: In the preceding paper in a series of the present thesis, a summary of the sea ice conditions off the coast of Hokkaido has been presented and the drifting route of ice has been estimated in one of its items (WATANABE, 1963 a). Here in the present paper is reported some velocities of drift ice along the estimated drifting route which have been measured by a new method of tracing some ice masses or icy eddies on successively observed ice charts by a kind of aerial photogrammetry (WATANABE, 1961). Furthermore, is given a method of separately computing the wind-induced and current-induced drifts from the data of drift velocities successively measured about an ice mass or icy eddy. In the consequence of such measurements of drift velocities in fairly wide area and of the computations of the current-induced drifts which are nearly equal to the velocities of the sea current in the case of low closeness of ice, a general figure of the drifting route of ice and the sea current off the coast of Hokkaido in the Okhotsk Sea has been in some degrees made clear.

1. Introduction

Though the sea ice conditions are not so predominating in the neighbouring seas of Japan as in the Arctic region or Greenland area, it is still important for revealing secrets of the drift-ice behavior off Hokkaido which gives serious damages to the life and industries in every winter, to collect data of drift-ice velocities. However, there have been rather scarce data of drift velocities of ice off Hokkido. In the winters of 1930 and 1938, several sets of the data of drift velocities about some ice-fields have been collected off southern Sakhalin by an icebreaker, the Ōdomari, belonged to the former Japanese Navy (KURASHINA, 1961). T. FUKUTOMI and his collaborators (1951) measured the relative velocities of a small ice-floe and several floe-bergs to the surface sea water due to wind by theodolites set on the floes about 10 nautical miles off the coast of Hokkaido in

April of 1948. It seems to the author that these are main source of our available data of drift velocities of ice offshore up to date, though a lot of data inshore have been collected by the shore observations. Such scantiness of the data offshore is account for lack of our observation ship at present being capable of penetrating into ice area, except for the only icebreaker, the Sōya, made for the use of the Antarctic Expedition of 1956–1962.

Now, a trial measuring velocities of drifting ice has been made by the author in the aerial sea ice reconnaissance since 1957. In the operation, lots of ice charts have been made from aerial photographs by the method of photogrammetry described in the author's preceding paper (WATANABE, 1961). The ice charts are precise and detailed enough for measuring the displacement of each ice mass

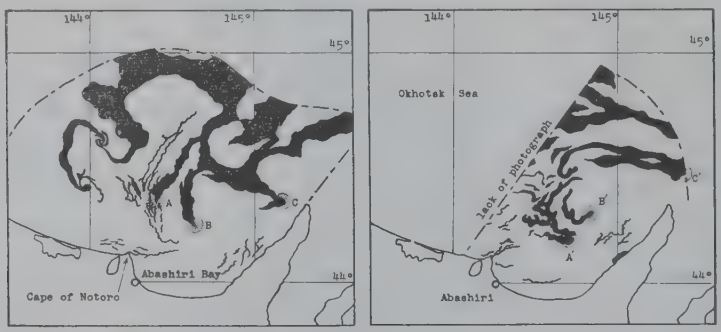

Fig. 1a (left) and 1b (right). Ice chart observed at nearly 1100 JST on Feb. 18, 1957, (1a) and the one at nearly 1000 JST on the next day (1b). The ice patterns consisted of small ice-floes and ice-cakes of the winter-ice are shown in blackened area (the areas of the new ice are uncharted here to aboid confusing the figures). Three tips of belts at A, B and C in Fig. 1a can be traced at A′, B′ and C′ in Fig. 1b. All ice charts in the present paper have been made by aerial photogrammetry.

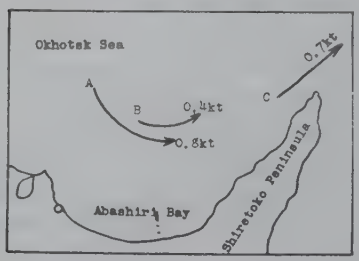

Fig. 2. Displacements of the ice masses during about 23 hours presented in the preceding figures. From the drift velocity 0.8 kt of the ice mass A, the existence of the sea current of about 0.8 kt in speed and the SE in direction near A has been estimated as in Table 2.

when they are made from aerial photographs taken on successive days in fine weather conditions and suitable ice states. Such sets of ice charts are rather few in the operation from 1957 to 1961, because of rare chance of fine weather conditions continued during two or three days under a suitable ice state. But the author could get three sets of the data on velocities of drift ice off the coast of Hokkaido. Here, in the present paper are reported the data together with a method separately computing the wind-induced and current-induced components from a set of drift velocities successively measured on an ice mass. Then the computed data of the drifts are discussed.

2. *Measured drift velocities*

When the ice area is poor in closeness and each stream or belt in it is separately recognizable on two ice charts successively observed at a suitable time interval, the displacements of ice masses traceable on each chart can be measured by comparing the two charts. One of such cases is illustrated in Figs. 1a, 1b and Fig. 2. In the chart on Feb. 18, 1957 (Fig. 1a) showing ice covers consisted of small ice-floes and ice-cakes of the winter-ice in blackened area, the ice pattern suggests the existence of sea current flowing off the coast, especially a considerably strong current off the Cape of Notoro—the location of the coast and the cape have been illustrated in the figures in the preceding paper (WATANABE, 1963 a). The successively observed ice chart on the next day is presented in Fig. 1b, where unfortunately the western half (left hand in the chart) has been uncharted by lack of photograph. Three tips of belts are traceable in these two charts which were observed at a time interval of about 23 hours. Deviding the amounts of their displacements by 23 hours, their average drift velocities during these two days are measured at 0.8 kt and 0.4 kt off the Abashiri Bay and 0.7 kt near the tip of the Shiretoko Peninsula as seen in Fig. 2. These vectors are just along the drifting route of ice estimated in the preceding paper.

When the closeness of ice is high, such tracing of each ice mass on successively observed two ice charts is hardly possible because of the complex pattern of ice cover and large deformation of each ice mass occurred in the time interval of the observations. But, if some noticeable icy eddies are seen in the charts, they are usefull for measuring drift velocity, since their lives seem to be long enough for tracing their displacements on successively observed ice charts in an adequate period. An example of such eddy method is illustrated in Figs. 3a, 3b, 3c and Fig. 4. Two icy eddies $\mathbf{A}_2$ and $\mathbf{D}_2$ are noticeable in the chart on Feb. 2,

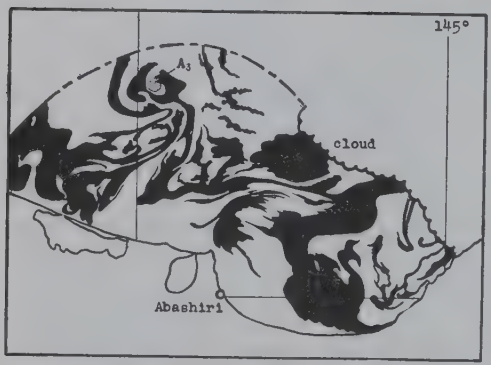

Fig. 3a (upper). Ice chart on Feb. 2, 1959.
Fig. 3b (middle). Ice chart on Feb. 3, 1959.
Fig. 3c (lower). Ice chart on Feb. 4, 1959.

It is rather difficult in complex patterns of ice as in these charts to trace the displacement of each ice mass on successively observed ice charts. However, the icy eddy is useful for measuring the drift velocity when it can be noticed among the complex pattern of ice. An icy eddy at A_2 seen in Fig. 3a is noticeable at A_3 in Fig. 3b, and then it can be traced at A_4 in Fig. 3c, From the displacements of the eddy A (namely, $A_2 \rightarrow A_3 \rightarrow A_4$) and the ones of more four eddies whose symbols are neglected in these charts in the sake of avoiding to confuse each ice pattern, seven vectors on ice drift have been made as illustrated in the succeeding figure.

1959 (Fig. 3a). They are traced at A_3 and D_3, respectively, in the chart on the next day (Fig. 3b) under the aid of inspecting the original aerial photographs

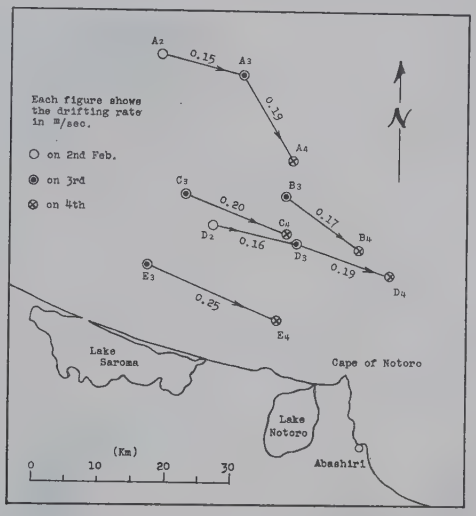

Fig. 4. Drift velocities measured by tracing five icy eddies presented in the preceding figures. From the drifts $A_2 \rightarrow A_3$ and $A_3 \rightarrow A_4$ of the icy eddy the wind-induced and the current-induced drifts have been separately computed as illustrated in Fig. 9.

used in making the two charts. More three eddies, B_3, C_3, E_3 can be picked up in the chart. Then, in the third chart of Fig. 3c observed on Feb. 4, 1959 these five eddies are recognized at A_4, B_4, C_4, D_4 and E_4, respectively. These symbols for the eddies are marked in Fig. 4 and neglected in the charts of Figs. 3a, 3b and 3c except for the eddy **A** (namely, A_2, A_3, A_4) in order to avoid making each ice pattern complex. Thus seven vectors of drift velocities have been measured as seen in Fig. 4 which may show the following characters. (1) Except for the vector $A_3 \rightarrow A_4$ during Feb. 3–4 the ice current directs nearly the ESE just along the coast. (2) The speeds are somewhat faster inshore than offshore. This suggests that the ice current tends to converge near the coast, especially off the Cape of Notoro as seen in Fig. 12 in the preceding paper. (3) The drift became faster during Feb. 3–4 than Feb. 2–3 as seen in comparing the vectors $A_3 \rightarrow A_4$ (0.19 m/sec in speed) and $D_3 \rightarrow D_4$ (0.19 m/sec) both during Feb. 3–4 to the vectors $A_2 \rightarrow A_3$ (0.15 m/sec) and $D_2 \rightarrow D_3$ (0.16 m/sec) during Feb. 2–3. Further-

more, the drift of the eddy A during Feb. 3–4 turned its direction right from the direction during Feb. 2–3. From the differences in speed and direction of the drift A, the author has been able to separately estimate the wind-induced drift and the current-induced drift as presented in the later section.

When the ice state is favorable, in other words, lots of noticeable ice masses or icy eddies can be plotted on successively observed ice charts, a velocity field of drifting ice masses in a fairly wide area can be made by the present method. In the ice charts of Fig. 5a and 5b observed on Feb. 18 and 19, respectively, in 1959, 22 ice masses can be traced under the aid of inspecting the original aerial photographs. Then a velocity field has been drawn as in Fig. 6, where each straight arrow is proportional to the average speed of ice drift during about 24 hours. Just similarly to the above-mentioned two cases each vector in this figure is along the drifting route estimated for the case of light ice period in the

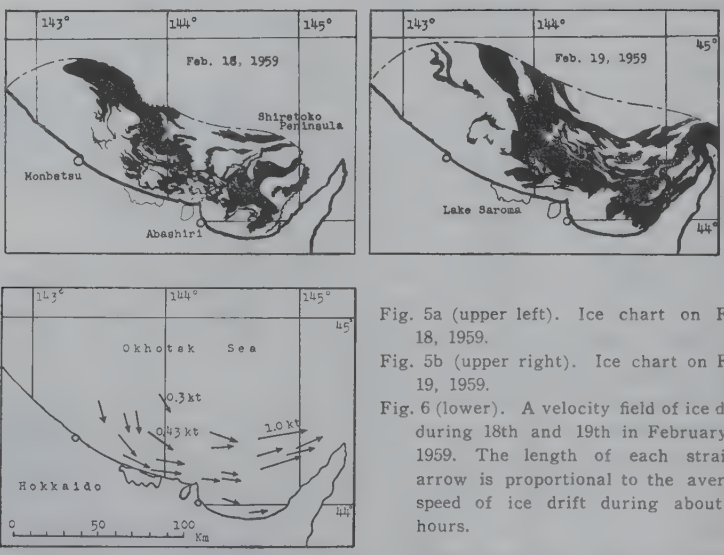

Fig. 5a (upper left). Ice chart on Feb. 18, 1959.

Fig. 5b (upper right). Ice chart on Feb. 19, 1959.

Fig. 6 (lower). A velocity field of ice drift during 18th and 19th in February of 1959. The length of each straight arrow is proportional to the average speed of ice drift during about 24 hours.

preceding paper, showing that the drift-ice coming from the north first directs the SSE-ward towards the coast near Lake Saroma with the speeds of 0.3 kt or lower, and runs along the coast with slightly increased speeds due to the convergence of the current, then flows towards the ENE off the Shiretoko Peninsula with

faster speeds of about 1 kt. This intensification in drift speed suggests that a strong convergence of the current occurs near the tip of the peninsula. Now, somewhat shorter vectors, namely of 0.25 kt or so in speed, are seen in the Abashiri Bay. They are accounted for the clock-wise whirl starting from the tip of the Cape of Notoro as illustrated in Fig. 7 which reduces the average speed of ice drift to a small amount even if each ice mass has a fairly large drift speed at each time. This kind of whirl was usually observed there as interestingly presented in Fig. 6a and 6b at page 54 in the author and his collaborator's former paper (WATANABE and NAKAYAMA, 1958).

Fig. 7. Ice chart in and near the Abashiri Bay on Feb. 25, 1957. The blackened area shows the one of very close accumulation of middle and large ice-floes, and ≡, |||| are the close and open area, respectively, of scattered small ice-floes and ice-cakes. This pattern represents the existence of a clook-wise whirl in the Abashiri Bay.

3. A method of separately computing the wind-induced and current-induced drifts

A wind blowing on the surface of an ice mass above the water level, that is called "local wind" in the present description, causes the ice's drift with a corresponding speed to the wind's one along such direction that deflects to the right from the wind's flowing direction due to the Coriolis force. The local wind induces not only such direct drift, but also an indirect drift to the ice mass that is caused by the surface current induced by the local wind in the surface layer in which the ice mass is immersed. Furthermore, the ice mass is driven also by the sea current, when it exists, independent of the local wind. Thence, the ice drift is subjected to the combined action of the local wind directly blowing on the surface of the ice above the water level, the surface current induced by the local wind, and the sea current independent of the local wind. In the following description, the ice drift caused directly and indirectly by the local wind is defined as the "wind-induced drift", and the one by the sea current independent of the local wind the "current-induced drift".

Now, leting the velocity of the local wind be **W**, its speed W and its direction φ which is measured in azimuth from the north as illustrated in Fig. 8, where

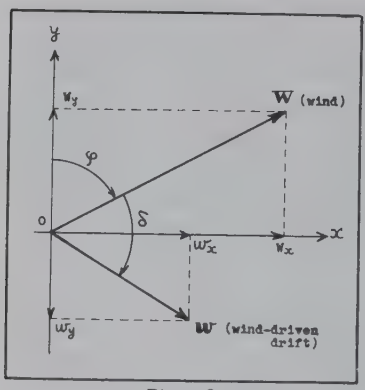

Fig. .8

the x-axis represents the direction to the east and the y-axis to the north, the two components W_x and W_y of the wind velocity are written as

$$W_x = W \sin \varphi, \qquad W_y = W \cos \varphi .$$

In accordance with the general view on ice drift that a speed w of the wind-induced drift is approximately proportional to the one W of the local wind, we can consider that the ratio $w/W \equiv k$, which is called the wind-factor, is nearly constant in a limit of W of not so large. Then, the velocity of the wind-induced drift of ice denoted by $\boldsymbol{w}$ (w_x, w_y) is developed as

$$w_x = w \sin(\varphi+\delta) = k \cos\delta \cdot W \sin\varphi + k \sin\delta \cdot W \cos\varphi ,$$
$$w_y = w \cos(\varphi+\delta) = k \cos\delta \cdot W \cos\varphi - k \sin\delta \cdot W \sin\varphi ,$$

where δ is the deflection angle of the ice's drift measured from the direction of the local wind as illustrated in Fig. 8. Leting

$$k \cos\delta \equiv l , \qquad k \sin\delta \equiv m , \tag{1}$$

we have

$$\left.\begin{aligned} w_x &= l W_x + m W_y , \\ w_y &= l W_y - m W_x . \end{aligned}\right\} \tag{2}$$

As mentioned above, the ice drift denoted by $\mathbf{D}$ (D_x, D_y) is a vector sum of the wind-induced drift $\boldsymbol{w}$ and the current-induced drift denoted by $\mathbf{C}$ (C_x, C_y), namely $\mathbf{D} = \mathbf{C} + \boldsymbol{w}$. Thence,

$$\left.\begin{aligned} D_x &= C_x + w_x = C_x + l W_x + m W_y , \\ D_y &= C_y + w_y = C_y + l W_y - m W_x . \end{aligned}\right\} \tag{3}$$

If there is a set of successively measured two or more values of drift velocities about an ice mass as mentioned in the preceding section, $\mathbf{C}$ and $\mathbf{D}$ can be separately determined. Considering $\mathbf{D}$ to be a measured velocity of an ice mass at a time under a local wind of $\mathbf{W}$, and $\mathbf{D}'(D_x', D_y')$ the velocity of the same ice mass under a local wind of $\mathbf{W}'(W_x', W_y')$ at the time after an adequate time interval from the former time, we make the difference between the two drift velocities in eliminating the unknown factors C_x, C_y. That is,

$$D_x - D_x' = l(W_x - W_x') + m(W_y - W_y') ,$$

$$D_y - D_y' = l(W_y - W_y') - m(W_x - W_x') .$$

Then we have

$$\left.\begin{aligned} l = k\cos\delta &= \frac{(D_x - D_x')(W_x - W_x') + (D_y - D_y')(W_y - W_y')}{(W_x - W_x')^2 + (W_y - W_y')^2} , \\ m = k\sin\delta &= \frac{(D_x - D_x')(W_y - W_y') - (D_y - D_y')(W_x - W'_x)}{(W_x - W_x')^2 + (W_y - W'_y)^2} . \end{aligned}\right\} \qquad (4)$$

Thus we can compute the wind-factor k and the deflection angle δ on the wind-induced drift of the ice mass by the following equations,

$$k = \sqrt{l^2 + m^2} , \qquad \tan\delta = m/l . \qquad (5)$$

Furthermore, using the measured values D_x, D_y of the ice's drift and the measurable values W_x, W_y of the local wind, and the values of l, m calcurated by the equation (4), we can compute the current-induced drift **C** as

$$\left.\begin{aligned} C_x &= D_x - (lW_x + mW_y) , \\ C_y &= D_y - (lW_y - mW_x) . \end{aligned}\right\} \qquad (6)$$

Here, it should be noticed that **C** is not always equal to the velocity of sea current itself, but is the drift velocity of ice induced by the sea current. In other words, **C** becomes nearly equal to the velocity of sea current when ice masses are scattered, but may be weakened in some degrees when the closeness of ice cover is high.

4. Practical computation of a wind-factor and a deflection angle of the wind-induced drift

The method described in the preceding section is applicable for the data of ice drift measured during Feb. 2–3 and Feb. 3–4 in 1959 presented in Fig. 4. The drift velocity of the icy eddy **A** is 0.15 m/sec in mean speed and N 103° in mean direction in the drift during from 2nd to 3rd, and 0.19 m/sec and N 145° during from 3rd to 4th in the month. Then the amounts of D_x, D_y, D_x' and D_y' are obtained as presented in Table 1. Since there was no directly observed datum on the local wind actually acted on the surface of the icy eddy, the author has estimated the wind velocities at 6.8 m/sec in mean speed and N 20° in mean direction during from 2nd to 3rd and at 8.4 m/sec and N 110° during from 3rd to 4th in February of 1959, from the geostrophic wind measured on the weather maps at 0900, 1500 and 2100 JST on Feb. 2, 0300, 0900, 1500 and 2100 JST on Feb. 3, and 0300, 0900 JST on Feb. 4. Then the amounts of W_x, W_y, W_x' and W_y' for the local wind are obtained as presented also in Table 1. Using these

Table 1. Amounts of the measured drifts and the estimated winds for computation.

	During 2nd and 3rd, Feb.		During 3rd and 4th, Feb.	
Measured drift (m/sec)	$D_x=0.142$	$D_y=-0.032$	$D'_x=0.109$	$D'_y=-0.155$
Estimated wind (m/sec)	$W_x=3.4$	$W_y=5.8$	$W'_x=8.0$	$W'_y=-2.9$

amounts a wind factor and a deflection angle have been computed by the equations (4) and (5) as

$$k=0.013\,,\qquad \delta=43^\circ\,, \tag{7}$$

and the current-induced drift by the equation (6) at 0.88 m/sec or about 0.16 kt in speed and N 130° or about the SE in direction.

The amount of $k=0.013$ seems somewhat smaller in comparing with the normal amount of 0.02 given by N. N. Zubov (1945) on the basis of Nansen, Sverdrup and other explorer's observations. The latter is the wind-factor of the polar pack at farther distance from shore in the Arctic Sea where the wind-induced drift seems to be able to normally behave without any shore effect. However, the former is the one of the winter-ice about 40 km off the coast of Hokkaido where the wind-induced drift is considered to be weakened in some

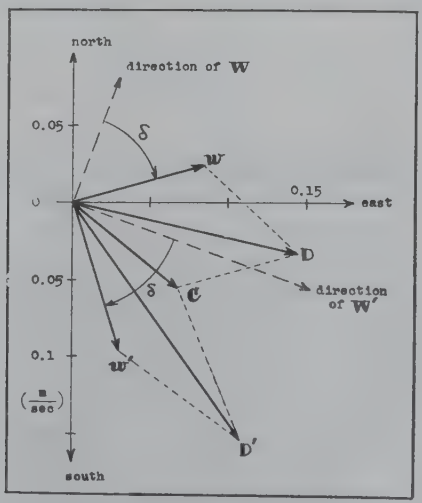

Fig. 9. Relation among the measured drifts and the computed wind-induced and computed current-induced drifts.

degrees from its normal drift in the influence of the shore as easily understood from the ice patterns in Fig. 3a, 3b, and 3c.

Besides such shore effect, the wind-factor varies with the shape and surface condition of drift-ice as seen in the data of ice drift measured by T. FUKUTOMI and his collaborators (1951) and in T. FUKUTOMI's theoretical investigations on the ice drift (1951a, 1951b, 1952, 1958). Furthermore, it varies also with the closeness of ice and by the intensity of the local wind. For instance, after Terence ARMSTRONG's review of Soviet works on sea-ice forecasting (1955), D.B. KARELIN and his collaborator has described that the volocity of wind-induced drift in lower closeness of 1/10~2/10 is about thrice the one in higher closeness of 9/10, and V.V. SHULEYKIN has given $k \fallingdotseq 0.01$ and $\delta \fallingdotseq 60°$ for the drift under weak wind whereas $k \fallingdotseq 0.025$ and $\delta \fallingdotseq 30°$ under strong wind.

In order to appreciate the reliability of the amounts $k=0.013$ and $\delta=43°$ computed above, Fig. 9 is presented for the relation among the vectors **D** and **D'** of the measured drifts, $\boldsymbol{w}$ and $\boldsymbol{w}'$ of the wind-induced drifts computed from the estimated local wind **W** and **W'** using $k=0.013$ and $\delta=43°$, and **C** of the computed current-induced drift. In this relation, a set of three vectors of $\overline{\mathbf{O}\boldsymbol{w}}$, $\overline{\mathbf{OD}}$ and $\overline{\mathbf{OC}}$ makes nearly up a parallelogram **O*w*DC** and another set of three vectors of $\overline{\mathbf{OC}}$, $\overline{\mathbf{OD'}}$ and $\overline{\mathbf{O}\boldsymbol{w}'}$ another parallelogram $\mathbf{OCD'}\boldsymbol{w}'$, namely $\mathbf{D} \approx \boldsymbol{w} + \mathbf{C}$ and $\mathbf{D'} \approx \mathbf{C} + \boldsymbol{w}'$ are nearly formed which show that the computed values of the wind-induced and the current-induced drifts are approximately correct.

Finally, the sea current off the Abashiri Bay in the middle of February in 1957 can be assumed from the velocity of drift towards N 120° with a speed of about 0.8 kt or 0.4 m/sec presented in Fig. 2. The drifts of ice masses at **A**, **B** and **C** are considered to have freely followed to the combined action of the local wind and the sea current in this case, because the closeness of ice was rather low and the area between the ice masses and the shore was completely opened as seen in the ice patterns in Figs. 1a and 1b. Thence, the wind-factor about the ice mass at **A** can be reasonably assumed at 0.02 or more, and the deflection angle at 30° or so. Multiplying the mean wind velocity observed at Abashiri by a factor of 1.5, a mean velocity of the local wind acted on the ice mass **A** during the time interval of 23 hours in which the ice patterns in Figs. 1a and 1b were successively observed can be approximately assumed at 9 m/sec in speed and N 50° in blowing direction. Thus from these amounts, two velocities have been computed for the wind-induced drifts in two cases of $k=0.02$ and

$k=0.04$ under a same amount of deflection angle $\delta=30°$ as in Table 2. As the two velocities of the current-induced drift in the table do not differ so much from each other, the ice mass **A** in Figs. 1a and 1b is considered to have been drifting towards nearly the SSE with a speed of about 0.4 m/sec or 0.8 kt. Furthermore, this velocity is to be nearly equal to the one of the sea current itself, because no factor weakening the current-induced drift from the velocity of sea current existed in this case where the closeness of ice was sufficiently low and then the shore effect was very weak as mentioned above.

Table 2. Estimated wind-induced and current-induced drifts of the ice mass **A** presented in Fig. 2 ($\delta=30°$ is used).

Given wind-factor (k)	0.02	0.04
Wind-induced drift	N 50°, 0,18 m/sec	N 50°, 0.36 m/sec
Current-induced drift	N 145°, 0.37 m/sec	N 170°, 0.42 m/sec

Considering the estimated velocities of the sea current as in Table 2 and the measured data on ice drift as in Figs. 2, 4 and 6 together with the drifting route of ice estimated in the preceding paper, it may be allowed to say on the sea current off the coast of Hokkaido in the Okhotsk Sea, that a sea current independent of the local wind flows southward or SSE-ward from the east offing of southern Sakhalin towards the coast of Hokkaido and runs nearly southeast-ward along the coast with a speed of 0.8 kt or so off the Cape of Notoro, then flows out ENE-ward off the tip of the Shiretoko Peninsula. This sea current will be shown in the succeeding paper in the present thesis (WATANABE, 1963b) to be an end flow of the East Sakhalin Current which is intensified in winter season, whereas it has been hitherto said not to flow in the southern region of the Okhotsk Sea.

Acknowledgment: The author wishes to express his sincere thanks to Dr. Kazuhiko TERADA of the Japan Meteorological Agency and Mr. Zen'ichi YASUI of the Hakodate Marine Observatory for their constant encouragement during this work.

References

ARMSTRONG, T. (1955): Soviet works on sea-ice forecasting. *Polar Record*, **7** (49), 302–311, Jan. 1955.

FUKUTOMI, T. (1951a): Study of sea ice XIII. Theoretical study on the steady drift of ice due to wind in the sea of small ice percentages (in Japanese). *Low Temp. Sci.*, **7**,

11–23.

—— (1951b): Study of sea ice XIV. On the steady drift current and steady drift of sea ice due to wind in frozen sea (in Japanese). ibid., 7, 25–37.

—— (1952): Study of sea ice XVIII. Drift of sea ice due to wind in the Okhotsk sea, especially in its southern part (in Japanese). ibid., 9, 137–144.

—— (1958): A theory on the steady drift on sea ice due to wind on the frozen sea. Artic Sea Ice. Nation. Acad. Sci.—Nation. Res. Coun., 223–236.

FUKUTOMI, T., K. KUSUNOKI and T. TABATA (1951): Study of sea ice XII. Some measurements of the wind pressure drift of sea ice (in Japanese). *Low Temp. Sci.*, **6**, 85–93.

KURASHINA, S. (1961): The data of sea ice observed by the former Japanese Navy from 1930 to 1943 (in Japanese). A mimeographed print issued by Hydrographic Division of Japan Maritime Safety Agency, 1–33.

WATANABE, K. and I. NAKAYAMA (1958): Results of non-vertical aerial photographic survey of sea-ice in the southwestern region of the Okhotsk Sea (in Japanese). *Memoirs of Japan Meteor. Agency*, **40** (1), 49–77.

WATANABE, K. (1961): On the theory and technique of an easy method of wide range photogrammetry for the observations of sea ice distribution. *Oceanogr. Mag.*, **12** (2), 77–121.

—— (1963a): Summary of sea ice conditions off the coast of Hokkaido,—Study on sea ice in the Okhotsk Sea (I). ibid., **14** (1).

——(1963b) On the reinforcement of the East Sakhalin Current preceding to the sea ice season off the coast of Hokkaido,—Study on sea ice in the Okhotsk Sea (IV). ibid., **14** (2).

Зубов. Н. Н. (1945): Льды Арктики, Глава XI,Ветер и дрейФ льдов (Ice in the Arctic Sea, Chapter XI, Drift of ice). Издательство Главсевморпути, Москва, p, 272.

The Oceanographical Magazine
Vol. 14. No. 1, November 1962

Storm Surge Forecasting Method and Telemetering, Recording, Printing and Indicating System of Tide and Other Elemements—so called "Call System"—in Japan

By

Kazuhiko Terada, Hidetaka Futi and Masamori Miyazaki

Japan Meteorological Agency

(Received October 31, 1962)

Contents

1. Storm surge forecasting method
2. Telemetering, recording, printing and indicating system of tide and other elements—so called "Call System"
   - 2.1 Measuring system
   - 2.2 Construction of equipment
     - (1) Central station equipment
       - (i) Control equipment
       - (ii) Radio equipment
       - (iii) Printing equipment
       - (iv) Indication equipment
     - (2) Observation office
       - (i) Control equipment
       - (ii) Radio set
       - (iii) Primary measuring instrument
   - 2.3 Specification of this equipment
     - (1) Supervising ability
     - (2) Ambient temperature
     - (3) Power source
     - (4) Telemetering interval
     - (5) Signal transmission system
     - (6) Observation speed
     - (7) Radio
     - (8) Primary instrument
3. Call system of Tokyo Bay
   - 3.1 Construction of the system
   - 3.2 Observed elements
   - 3.3 Operation

1. Storm surge forecasting method

Japan is frequently attacked by the severe typhoon causing various damage over the coastal regions of Japan, specially at the inner part of the bay directed open to the south. The severe damage is deeply connected to the storm surge.

Up to the recent years the following experimental formulae have been used for the forecasting of the height of tide due to the storm surge.

$$h = a\,\Delta p + bw^2 \cos\theta + (c),$$

where

h: meteorological tide (cm),

Δp: (monthly mean pressure)—(minimum pressure of typhoon) (mb),

θ: angle between the direction of longitudinal axis of bay and the actual wind direction,

w: wind velocity (m/s),

a, b, c: constant.

From the observational data of tide, pressure, wind direction and wind velocity, magnitudes of a, b and c were obtained as shown in Table 1. Also in Table 2 data of tidal condition in Japan are listed.

The above formulae were obtained empirically from the data at one point and so such formulae have been utilized only for the rough estimation of storm surge. In order to have more reliable value of storm surge, it is necessary to treat the phenomena as three dimensional phenomena. To do so we have utilized the electronic computor IBM-704 which was installed in the Japan Meteorological Agency several years ago.

In 1959 we have experienced the great damage due to storm surge by Ise Bay typhoon. Then we were forced to hurry up to investigate the phenomena of such storm surge. Main causes of these surges are strong winds with generation of tangential stresses exerting on horizontal surface and atmospheric pressure anomalies accompanied with the disturbances. Besides, in coastal area, we experience considerably the effects of the incoming water from the center of disturbance, the coastal reflection, and the damping by bottom topographies. Effects of these factors were numerically estimated and introduced for the numerical calculation as the functions of known quantities or as the results of known dynamic processes.

In case of Ise Bay typhoon we have calculated the distribution of storm surge

Table 1. Value of constants.

$h=a\Delta p+bw^2\cos\theta+(c)$

Name of Station	a	b	c	Main Wind Direction	Number of Observation
Abashiri	1.82	0.08		NE	
Hakodate	1.03	0.16		SW	
Hachinohe	1.429	0.015		ENE	7 (1957～60)
Miyako	1.193	0.012		NNW	6 (1958～60)
Ayukawa	1.346	0.020		SE	9 (1945～59)
Onahama	0.700	0.083		N	8 (1956～59)
Choshi	0.622	0.056		SSW	6 (1951～59)
Mera	1.935	0.012		SW	7 (1957～60)
Tokyo	1.059	0.138		S 7.0° E	13 (1944～60)
Ito	0.725	0.005		SW	5 (1951～59)
Uchiura	1.435	0.021		SW	3 (1951～59)
Shimizu	0.566	0.052		SSW	3 (1953～59)
Omaesaki	0.986	0.009		SW	3 (1958～59)
Maisaka	1.845	0.067		SE	5 (1953～59)
Nagoya	1.674	0.165		SSE	11 (1952～55)
Toba	1.825	0.001		ESE	7 (1950～59)
Uragami	2.284	0.025		SE	6 (1950～61)
Kushimoto	1.490	0.036		S	10 (1950～60)
Shimotsu	2.000	0.022		SSW	13 (1934～60)
Wakayama	2.608	0.003		SSW	12 (1950～60)
Tannowa	2.552	0.004		SSW	8 (1953～60)
Osaka	2.167	0.181		S 6.3° E	28 (1929～53)
Kobe	2.330	0.114		S 31.2° W	31 (1926～54)
Sumoto	2.281	0.026		SSE	10 (1950～60)
Uno	4.109	−0.167		WNW	8 (1950～60)
Kure	3.730	0.026		E	4 (1951～56)
Komatsujima	1.720	0.019		SE	10 (1951～60)
Takamatsu	3.184	0.000		SE	9 (1950～60)
Matsuyama	4.303	−0.082		SSE	7 (1950～56)
Uwajima	2.330	−0.012		SSE	7 (1950～56)
Tosashimizu	1.428	0.022		S	10 (1950～57)
Kochi	2.385	0.033		SSE	8 (1950～60)
Shimonoseki	1.231	0.033		ESE	10
Tomie	1.094	0.027		SE	5
Megami	1.175	0.054		WSW	6
Misumi	1.185	0.154		SSW	11
Makurazaki	0.973	0.040		S	4
Kagoshima	1.234	0.056		SSE	6
Aburatsu	1.005	0.036		SE	6
Tonoura	1.17	+0.021	−12.9	NNW	6
Sakai	0.48	+0.027	+15.4	ENE	6
Miyazu	1.43	−0.014	− 4.8	NE	14

Table 2. Tidal condition in Japan.

Name of Tidal Station	Period of Observation	Standard Mean Sea Level of Tokyo Bay	Mean Sea Level of Recent 5 Years	Mean High Water Springs	Mean Low Water Springs	Maximum High Water Level	Minimum Low Water Level
Wakkanai	1955～1960	1.478	1.656	1.881	1.462	2.300	1.080
Abashiri	1957～1960	1.415	1.444	2.076	0.882	2.390	0.530
Hanasaki	1954～1960	2.004	2.128	2.760	1.339	3.999	0.370
Kushiro	1947～1960	1.389	1.447	2.027	0.648	3.460	−2.600
Hakodate	1956～1960	1.350	1.446	1.911	0.922	3.580	−1.570
Aomori	1956～1960	0.702	1.006	1.415	0.583	1.760	0.240
Hachinohe	1937～1960	0.505	0.714	1.307	−0.054	3.650	−2.150
Miyako	1938～1960	1·006	1.156	1.748	0.354	2.170	−0.210
Ayukawa	1938～1960	1.544	1.678	2.302	0.861	4.250	−1.930
Onahama	1951～1960	1.364	1.448	2.038	0.714	3.750	−1.290
Choshi	1955～1960	1.107	1.049	1.661	0.266	2.270	−0.180
Mera	1957～1960	1,246	1.229	1.864	0.338	3.627	0.060
Tokyo	1951～1960	1.800	1.828	2.717	0.697	3.420	0.270
Kawasaki	1954～1960	1.371	1.461	2.289	0.348	2.870	−0.050
Yokohama	1959～1960	1.747	1.764	2.441	0.559	2.940	0.020
Okada	1953～1960	—	1.572	2.213	0.698	2.880	0.310
Ito	1935～1960	2.123	2.100	2.736	1.258	3.140	0.740
Shimizu	1937～1960	1.658	1.611	2.336	0.697	3.030	0.250
Omaesaki	1952～1960	1.434	1.430	2.154	0.507	2.960	−0.100
	1959～1960	1.647	1.623	2.344	0.686	3.660	−0.500
Maisaka	1936～1960	0.792	0.561	1.038	0.132	2.740	−0.240
Nagoya	1949～1960	1.992	2.043	3.204	0.644	5.810	0.040
Toba	1926～1960	2.560	2.493	3.354	1.454	4.450	0.900
Owase	1953～1960	1.739	1.582	2.331	0.578	3.220	0.220
Uragami	1939～1960	1.693	1.452	2.236	0.493	3.460	0.110
Kushimoto	1925～1960	1.831	1.707	2.498	0.690	3.110	0.320
Shimotsu	1926～1960	1.886	1.964	2.771	1.105	3.650	0.560
Wakayama	1949～1960	1.022	1.102	1.924	0.083	2.760	−0.400
Tannowa	1935～1937 1943～1960	1.806	1.900	2.598	1.016	3.100	0.270
Osaka	1939～1960	2.772	2.944	3.651	2.063	4.690	1.170
Kobe	1926～1960	1.163	1.321	2.012	0.461	2.960	−0.400
Sumoto	1941～1960	1.693	1.867	2.517	1.082	3.180	0.290
Uno	1951～1960	1.433	1.674	2.801	0.429	3.470	−0.020
Kure	1952～1960	2.354	2.619	4.328	0.661	5.140	0.050
Shimonoseki	1951～1960	2.459	2.582	3.694	1.096	4.240	0.620
Matsuyama	1950～1960	2.247	2.322	3.950	0.500	4.750	−0.060
Takamatsu	1949～1960	1.727	1.921	2.987	0.730	3.670	0.100
Komatsujima	1951～1960	1.807	1.959	2.737	0.997	3.320	0.390
Kochi	1950～1960	1.314	1.192	2.033	0.129	2.830	−0.440
Tosashimizu	1931～1960	1.802	1.702	2.552	0.647	3.240	−0.170

Name of Tidal Station	Period of Observation	Standard Mean Sea Level of Tokyo Bay	Mean Sea Level of Recent 5 Years	Mean High Water Springs	Mean Low Water Springs	Maximum High Water Level	Minimum Low Water Level
Uwazima	1927～1960	2.161	2.206	3.186	1.007	3.880	0.430
Aburatsu	1930～1960	1.443	1.492	2.362	0.393	3.020	−0.200
Kagoshima	1948～1960	2.024	2.027	3.330	0.537	4.840	0.020
Makurazaki	1956～1960	2.702	2.700	3.889	1.296	4.280	0.910
Minamata	1932～1960	—	3.217	4.817	1.453	5.290	0.990
Misumi	1936～1960	3.836	4.202	6.074	2.123	6.860	1.280
Megami	1950～1960	2.384	2.463	3.802	0.851	4.440	−0.330
Fukaura	1957～1960	3.512	3.550	3.891	0.938	4.470	0.380
Tomie	1953～1960	—	2.662	3.954	1.126	4.430	0.620
Tonoura	1925～1960	0.833	1.048	1.368	0.789	2.060	0.260
Sakai	1932～1960	1.143	1.317	1.499	1.135	2.120	0.630
Saigo	1959～1960	1.102	1.010	1.213	0.791	1.600	0.470
Miyazu	1953～1960	0.863	1.084	1.284	0.885	1.710	0.570
Iwasaki	1947～1960	1.292	1.664	1.891	1.447	3.060	1.050

These values are measured from the individual datum line of respective tidal station.

along the coast of Ise Bay and the feature of time sequence of tidal phenomena. And the calculated values are compared to the observed values of storm surge and we found that there are good coincidences between them, which allows the above assumptions of various factors to be of rather reliable nature.

Theoretically speaking we can calculate numerically the feature of storm surge at various places using the electronic computor. But this calculation should be done under the assumption that the feature of typhoon is perfectly anticipated.

So if the typhoon is forecasted, we might be able to calculate the feature of storm surge in routine basis and this process is, ideally, preferable for the routine works of forecasting of storm surge.

But as an actual problem such ideal process is not able to be done. So we must confine ourselves to calculate the feature of storm surge by assuming various types of typhoon, for example, typhoon path, strength, velocity, wind velocity distribution etc. If we have the results of the calculation of various assumed typhoon, then we may anticipate the feature of storm surge comparing the forecast of typhbon now attacking our country. So it will preferable, in the first case, to calculate the feature at the most important port of Japan. Now we have listed some of the most disastrous surges in Tokyo Bay, Osaka Bay and Ise Bay, where are often strucked by heavy typhoon surges in Japan.

So we have computed storm surges caused by various possible severe typho-

Table 3. Values of heavy storm surges in Tokyo Bay, Osaka Bay and Ise Bay.

Bay		Typhoon		Track and Depth*			Maximum Surge Height (m)
Location	Opening to	Name	Date	Area	Direction	Depth (mb)	
Tokyo Bay	SSW	—	Oct. 1, 1917	50 km NW of the Bay	NE	950	2.3
Osaka Bay	SW	Muroto	Sept. 21, 1934	West coast	NE	950	3.1
		Jane	Sept. 25, 1950	West coast	NNE	965	2.4
Ise Bay	SSE	Ise Bay	Sept. 26, 1959	50 km west of the Bay	NNE	945	3.4

* Data in the period of maximum surge.

ons as to the above mentioned bays. And when a typhoon became actually near to the coast of Japan, we select a typhoon model of above mentioned computation according to forecasted magnitude and course of a moving typhoon. Then we may be able to clarify the feature of storm surge as is shown in Fig. 1.

On other hand we are currently watching the variation of tide height, wind velocity, wind direction and pressure by the method described in section 2 and we can forecast qualitatively storm surge as to the whole bay by a modified form after checking the actual data of surge compared with the computed one caused by the typhoon model.

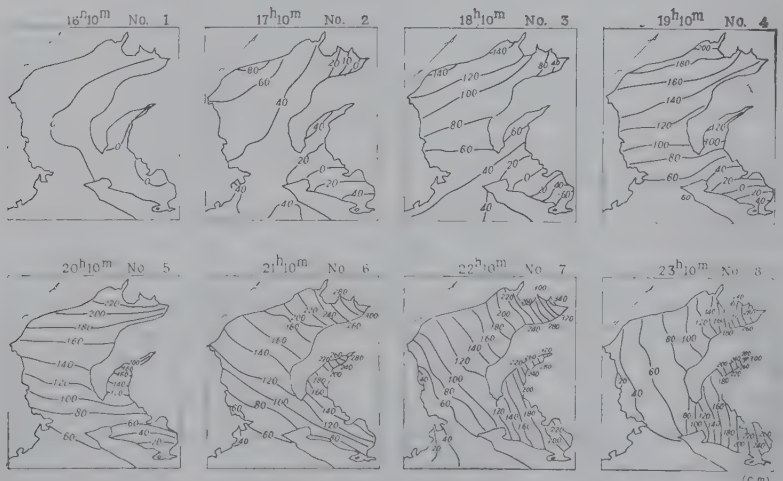

Fig. 1. The results of computed storm surge caused by Ise Bay Typhoon.

2. *Telemetering, recording, printing and indicating system of tide and other elements—so called "Call System"*

2.1. Measuring system

If, in the ordinay telemetering system (central station has many daughter stations) all measurements are to be performed simultaneously, the equipment of central station becomes very complex and large-scaled, and the using frequency band of transmission line (especially wireless route) becomes remarkably wide. To eliminate this point, telemetering is preferable to be performed by central calling, so far as the feature of data collection is allowed. That is after one daughter station had sent to central, the next station start to transmit by central calling signal. Hence, the central equipment is made very simple and economical. For the storm surge study, we applied such a scanning telemetering system named "Call System".

This equipment is used for two purposes=the one is the automatization of daily observation and the other the collection of continuous data in emergency. In the former, all observation offices are automatically called out to record their data in response to six stages from once a day to twenty-minutes interval. The time necessary to complete the measurements of all data depends upon the number of measuring items, but it is approximately 14 second per office for three observa-

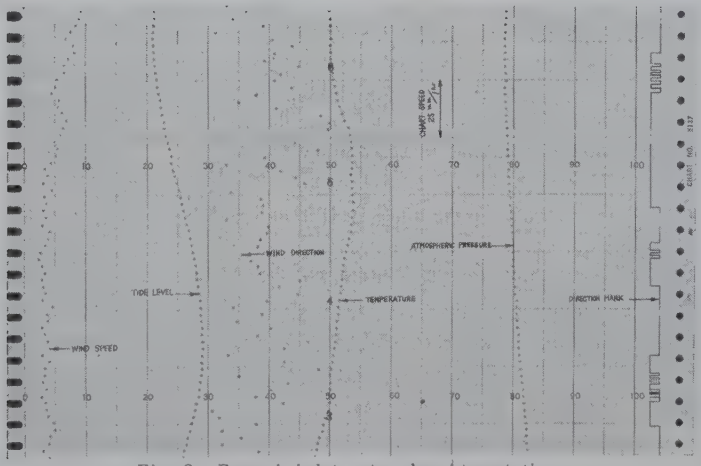

Fig. 2. Recorded data at a daughter station.

tion items. In case of obtaining continuous data of all places, observations are performed without interruption by making the call interval "continuous".

At each station, measuring items for instance wind direction, wind speed, tide level etc. are successively selected at 36 second interval and each data is automatically recorded by multi-color electronic recorder on roll paper. One of the recorded data in shown in Fig. 2.

The paper speed is changeable 25,50,100 mm/h. In case call signal is received from the central station, the electronic recorder stops recording. Then data are

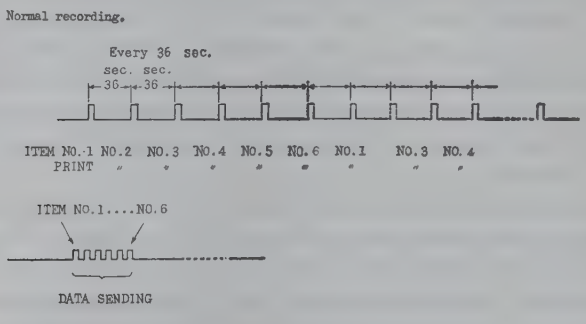

Fig. 3. Time-table of normal recording and data sending.

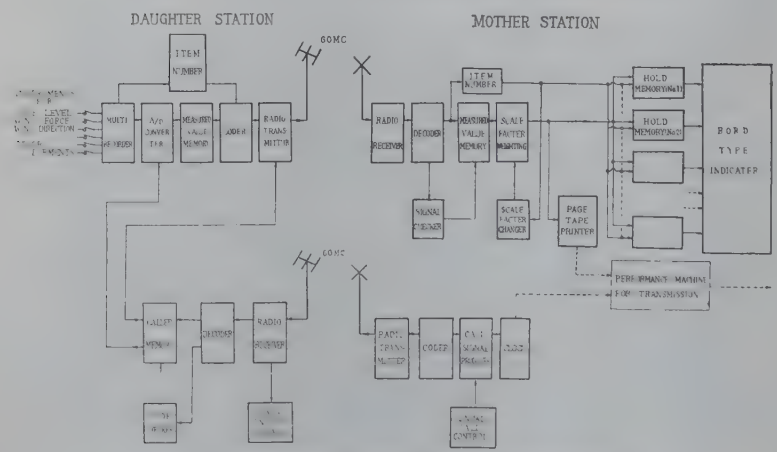

Fig. 4. Mother and daughter station block diagram.

sent to the telemetering equipment to convert digital number (for instance NNE, for wind-direction, 30 m/s for wind speed etc.) transmitted to the central station by 2.5 second/item over transmission line. Errors occuring during transmission are checked at the central station by parity inspection. In case mis-signals are found, calling signal are sent again to same daughter station to repeat the telemetering. When data-sending is completed in daughter station, transmitting equipment automatically stops and automatic recording starts again. Timetable of the above procedure is shown in Fig. 3 and Fig. 4 shows the block diagram of call system.

2.2. *Construction of equipment*

The central station has control equipment, radio set, printer and indication equipment, while the daughter station has control equipment, radio set, and primary measuring apparatus. Each of the above equipments is described as follows.

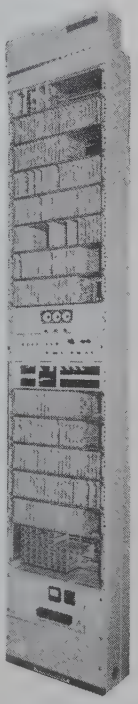

Fig. 5. Control equipment.

(1) *Central station equipment*

(i) *Control equipment*

This equipment controls to send the "CALL SIGNAL" to each daughter station at a definite time, and to print in a definite form and indicate on the indicating board panel all the data measured at every daughter station which have been mathematically treated. The equipment uses switching transistors and is composed of printed plates, whose size being 2,750 mm×520 mm ×225 mm. Its front view is shown in fig. 5.

(ii) *Radio equipment*

This is VHF FM one-channel wireless telephone equipment for composiong signal transmission route between the central station and each daughter station. The receiver being totally transistorized, has very long life and needs no maintenance. Its frequency is 60 Mc and its transmitting out-put is 25 W or 50 W The line-up is shown in Fig 6. Its size is 1,600 mm×520 mm× 225 mm. Its front view is shown in Fig. 7.

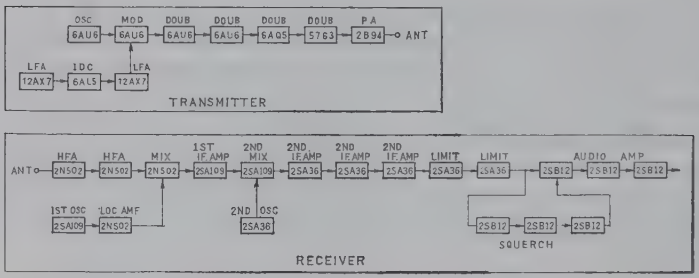

Fig. 6. Block diagram of equipment.

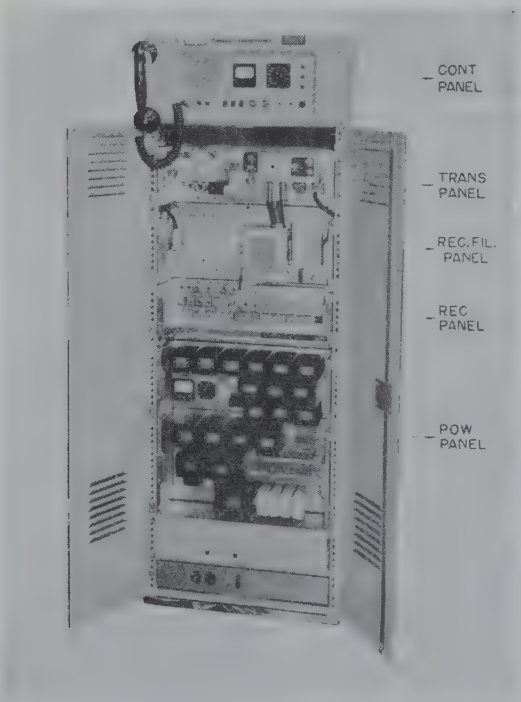

Fig. 7. Radio equipment.

(iii) *Printing equipment*

This is a electric type-writer which has been reconstructed out of a common

desk-type type-writer. Its external appearance is shown in Fig. 8.

(iv) *Indication equipment*

This equipment, having the size of 2,000 mm× 2,100 mm×350 mm, is used for indicating numerically the data of each place so as to be convenient for supervision. Its front is covered with glass plate for convenience of putting down such necessary items as isobaric-, iso-thermal lines, etc. Its external appearance is shown in Fig. 8.

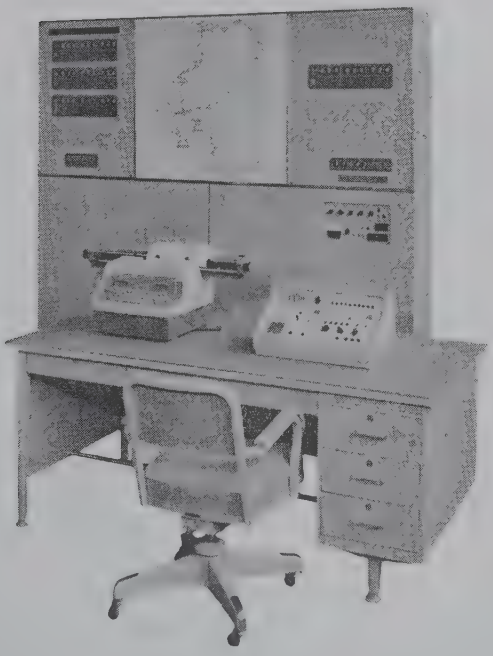

Fig. 8. Printing and indicating equipment.

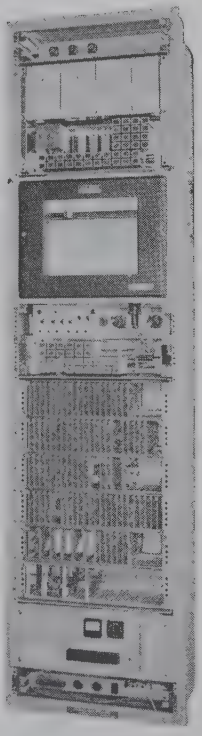

Fig. 9. Control equipment.

(2) *Observation office*

(i) *Control equipment*

This is an equipment, totally transistorized and composed of print plates,

which sends out measured data by receiving a calling signal from the central station. It has a half-enclosed structure with the dimension of 520 mm × 2,300 mm × 235 mm. Electronic recorder is included in this equipment for continuous recording. Its front view is shown in Fig. 9.

(ii) *Radio set*

This is same as that used for central station.

(iii) *Primary measuring instruments*

This is a converter used for changing such measured values as wind direction, wind speed, tide-level, etc., into electrical signals convenient for telemetering. Its principle lies in changing all measured values first into mechanical displacements and then converting them into A. C. voltages by means of differential transformer.

At the measuring heads of tide gauge, and barometer, changes of water and atmospheric pressure are converted into displacements by means of spring type primary converter (pressure to displacement), while at the trichlene-filled measuring head of thermometer, cubical expansion due to its thermal change is converted into displacement in the same way. As the differential transformer cores coupled with the above primary converters, are subject to displacements, they are changed into voltages.

In an anemoscope, displacement is given to the core of differential transformer through the direction cam fixed to the rotary shaft of a vane. In an anemometer, one pulse is generated every 100 m wind run by the three-cup anemometer and the generated pulses are integrated by the pulse-counter of wind-speed converter to give displacement to the core of differential transformer by means of the cam coupled with gear train. This pulse-counter is designed to obtain the mean wind speed for a period of ten minutes. Three sets of wind speed converter are used at five minute interval one after another to obtain the mean wind-speed for the past ten minutes.

The above electrical signals are given to the self-balancing recorder as its measurement input and recorded on the same papar with different colors. Furthermore, by use of mechanical analog-digital converter, fixed to the balancing motor shaft of the recorder, the above analog quantity is converted to digital one and given to the telemetering control circuit.

Fig. 10 shows the block diagram of the measuring system and Figs 11, 12, 13, 14, 15 show the measuring heads of anemoscope, anemometer, barometer,

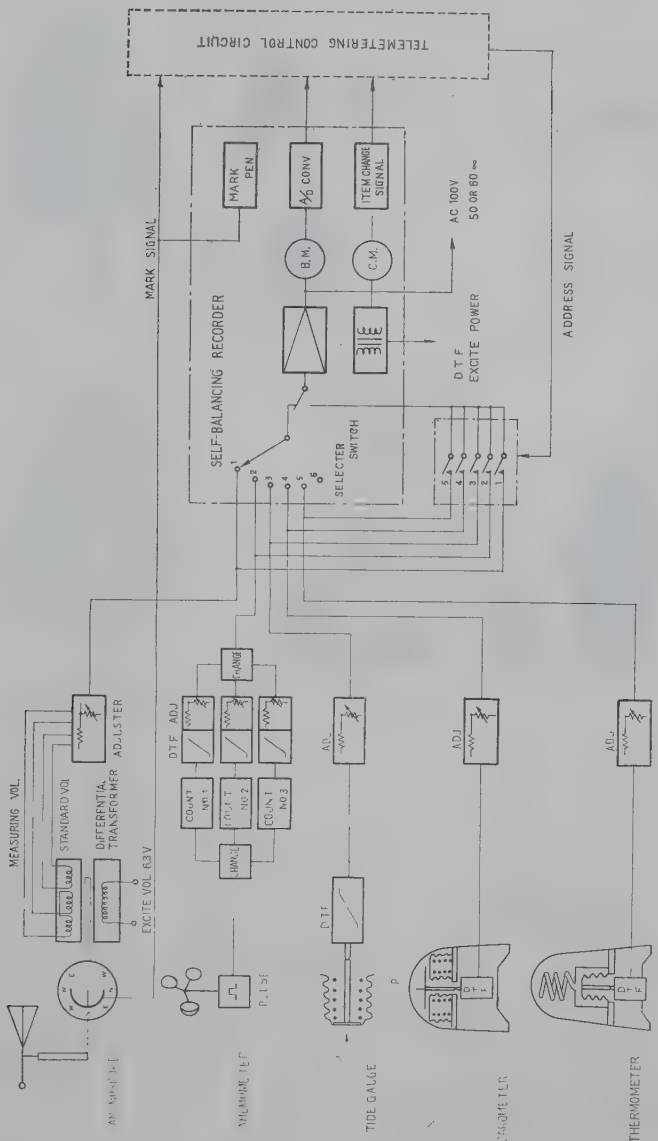

Fig. 10. Measuring system block diagram.

Fig. 11. Anemoscope.

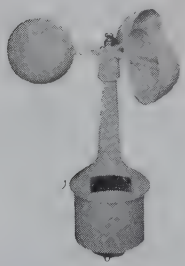

Fig. 12. Anemometer.

Fig. 13. Barometer.

Fig. 14. Tide gauge.

Fig. 15. Thermometer.

tide gauge, and thermometer.

2.3. Specification of this equipment

(1) Supervising ability: maximum ten observation offices (maximum six items per office)

(2) Ambient temperature: −10°C to +40°C.

(3) Power source: A.C.-single phase 100V±10 % or 200V±10%
400 VA per observation office
1 KVA per supervising office
In case of emergency, batteries can supply power source for more than ten hours.

(4) Telemetering interval
Automatic telemetering continuous

Once per 20 min, 30 min, 1h, 3h, 6h, 24h.
Manual telemetering
At any time

(5) Signal transmission system: decimal three-figure numerical transmission due to pulse-code modulation

(6) Observation speed: within 3.5 minutes for 10 observation office (six items. max)

(7) Radio

A. General characteristics

1. Frequency range: 54 Mc ... 68 Mc
2. Modulation: FM system
3. Frequency stability: less than ±0.002 %
4. Talk system: Press-talk system or Two-way system
5. Power supply: AC 100V/200V±5 %
6. Power comsumption

	Stand-by	Operate
Power output 25 W	70 W	300 W
50 W	70 W	350 W

7. Allowable range of Temperature : −10°C～+50°C
   of Humidity : 40 %～95 % (at 35°C)

B. Characteristics of Transmitter

1. Power output: 25 W or 50 W
2. Frequency multiplication: 16 times
3. Modulation
   Phase modulation by crystal control with I. D. C.
4. Spurious radiation
   In band: less than −80 db for carrier level
   Out of band: less than −60 db for carrier level
5. Maximum frequency deviation ±10 Kc
6. Modulation frequency to frequency deviation characteristics on 1 Kc basis
   −10.5±3 db at 0.3 Kc
   +4 ±3 db at 2.0 Kc
   +6 ±3 db at 3.0 Kc

7. Distortion factor
   Less than −20 db at 1 Kc 70% modulation
8. Output impedance: 50 Ω
9. Audio input impedance: 600 ohms or 50 ohms

C. Characteristics of Receiver

1. Receiving system: Double superheterodyne
2. Frequency of I.F: 1st I.F 4.3 Mc
   2nd I.F 455 Kc
3. S/N ratio
   (For 100% modulation at 1 Kc)
   More than 15 db at 0 dbμ input
   More than 35 db at 20 dbμ input
4. Squelch sensitivity
   Adjustable 0 dbμ.....+15 dbμ
5. Band width
   More than 20 Kc at 6 db down from center frequency
6. Selectivity
   Less than 50 Kc at 75 db down from center frequency
7. Spurious response
   Less than−80 db
8. Intermodulation characteristics
   More than 65 db for adjacent and alternate channel
9. Audio frequency characteristics on 1 Kc basis.
   +6 db±3 db at 0.3 Kc
   −4 db±3 db at 2.0 Kc
   −8 db±3 db at 3.0 Kc
10. Distortion factor
    Less than −20 db at 0.5 W output
11. Audio output impedance
    600 ohms
12. Audio output
    More than 0.5 W

(8) Primary Instruments

Name	Range	Accuracy
Anemoscope	16 direction	±5

Anemometer	0–60 m/s (10 minutes mean value)	less than 10 m/s ±0.5 m/s more than 10 m/s ±5%
Tide guage	0–10 m	±1.5% (for full scale)
Barometer	900–1,050 mb	±1 mb
Thermometer	−30°～+50°C	+1°C

3. *Call system of Tokyo Bay*

3.1. *Construction of the system*

This system is constructed with one mother station, four daughter stations and one relay station. Details of each station are shown in the follwing block diagram.

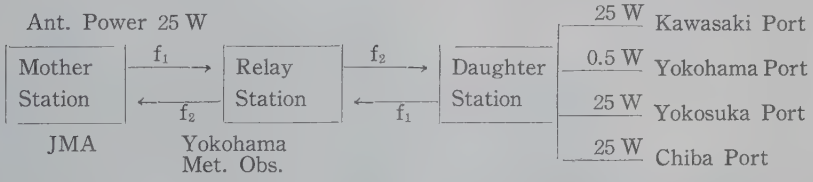

Type and frequency of waves are as follws:

f_1.....$26F_2$ $26F_3$ 61.19 Mc

f_2.....$26F_2$ $26F_3$ 63.02 Mc

3.2. *Observed element*

Observations at each daughter station are carried out on (1) wind direction (vane), (2) wind velocity (3-cup anemometer), and (3) tide level (water-pressure type tide guage). Actual observed values are used as the wind direction and tide level, and 10 minute averages for each 5-minute intervals are taken.

Changes of all element are all reduced to electric voltage changes. Since the electronic automatic balancing method are used, automatic records of each element are obtained at each daughter station.

3.3. *Operation*

These obtained values are converted into digital figures with an analog-digital converter, and are sent to the mother station as the pulse codes (1, 2, 4, 8, parity).

At the mother station, these plues codes are reduced into digital figures, and through the scale factor weighting true values are obtained. These are manifested on map board for each daughter station and element with nixie tubes. The

results are printed simulltaneously.

Calling from the mother station is divided into two ways, routine and optional calls. Routine calls are made simultaneously for all daughter stations with the intervals of 20-minute, 30-minute, 1-hour, 3-hour and 6-hour. Optional calls are made at any time for simultaneous (one after another), or individual (particular daughter station) basis with hand operation. Telephone communication is possible between the mother station and each daughter station and relay station, however, in this case operation of the telemetering system is suspended.

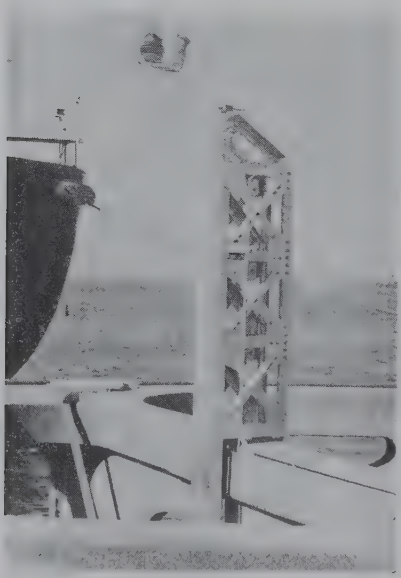

Fig. 16. Tide gauge at Yokohama Port.

Fig. 17. Anemometer, anemoscope and Yagi antenna at Kawasaki Port.

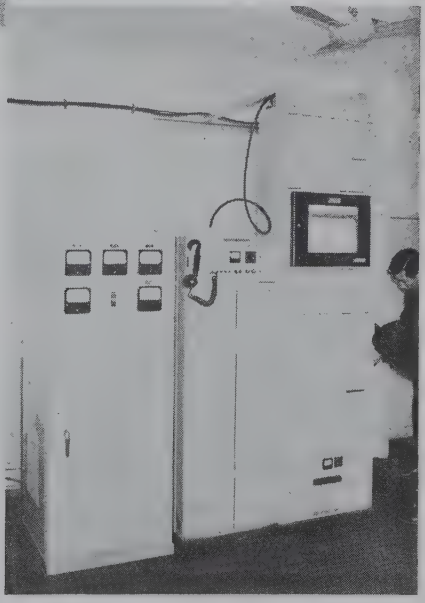

Fig. 18. Radio and control equipment at Kawasaki Port.

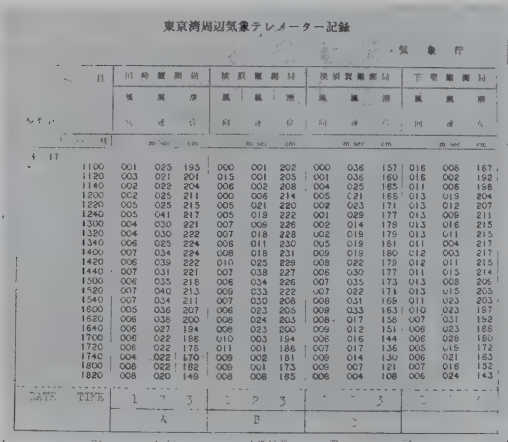

東京湾周辺気象テレメーター記録

日	川崎鶴見測候			横浜気象観測局			横須賀気象観測局			千葉観測局		
	風向	風速	潮位	風向	風速	潮位	風向	風速	潮位	風向	風速	潮位
		m/sec	cm		m/sec	cm		m/sec	cm		m/sec	cm
4 17												
1100	001	025	195	000	001	202	000	036	157	016	008	167
1120	003	021	201	015	001	205	001	036	160	016	002	192
1140	002	022	204	006	002	208	004	025	165	011	006	198
1200	002	025	211	000	006	214	005	021	168	013	019	204
1220	005	025	215	005	021	220	002	023	171	013	012	207
1240	005	041	217	005	019	222	001	029	177	013	009	211
1300	004	030	221	007	009	226	002	014	178	013	016	215
1320	004	030	222	007	018	228	002	019	179	013	011	215
1340	006	025	224	008	011	230	005	019	181	011	004	217
1400	007	034	224	008	018	231	009	019	180	012	003	217
1420	006	039	222	010	025	229	008	022	179	012	011	215
1440	007	031	221	007	038	227	006	030	177	011	015	214
1500	006	035	218	006	034	226	007	035	173	013	008	208
1520	007	040	213	009	033	222	007	022	171	013	015	205
1540	007	034	211	007	030	208	008	031	165	011	023	203
1600	005	036	207	006	023	205	009	033	163	010	023	197
1620	006	036	200	008	024	203	008	017	156	007	031	192
1640	006	027	194	008	023	200	009	012	151	006	023	188
1700	006	022	186	010	003	194	006	016	144	006	028	180
1720	006	022	178	011	001	188	007	017	136	005	015	172
1740	004	022	170	009	002	181	008	014	130	006	021	163
1800	006	022	162	009	001	173	009	007	121	007	016	152
1820	008	020	149	008	008	165	006	004	108	006	024	143
DATE	TIME	1	2	3	1	2	3	1	2	3	1	2	3
		A			B			C			D		

Fig. 19. Printed record at the Mother Station of JMA.

1: Wind Direction
2: Wind Velocity
3: Tidal Height
A: Kawasaki Port Station
B: Yokohama Port Station
C: Yokosuka Port Station
D: Chiba Port Station

References

MIYAZAKI, M., T. UENO and S. UNOKI (1961): Theoretical investigation of typhoon surges along the Japanese coast. *Oceanogr. mag.* 13 (1), 1961.

MIYAZAKI, M., T. UENO and S. UNOKI (1962): Theoretical investigation of typhoon surges along the Japanese coast. (II). *Oceanogr. Mag.* 13 (2), 1962.

MARINE DIVISION, JMA (1960): Investigations on storm surges produced by the Ise Bay Typhoon with some technical conditions. *Technical Report of the JMA*, No. 4, 1960. (in Japanese)

MARINE DIVISION, JMA (1960): Numerical investigations on storm surges in Tokyo Bay with some technical conditions. (in Japanese)

MARINE DIVISION, JMA and THIRD PORT AND HARBOUR CONSTRUCTION BUREAU, JMT (1961): Numerical investigation on storm surges in Osaka Bay with some technical conditions. *Technical Report of the JMA*, No. 11, 1961. (in Japanese)

MARINE DIVISION, JMA and FOURTH PORT AND HARBOUR CONSTRUCTION BUREAU, JMT (1962): Numerical investigations of storm surges in the western part of the Seto Inland Sea. *Technical Report of the JMA*, No. 16, 1962. (in Japanese)

TERADA, K. and H. FUTI (1962): Telemetering tide recorder and "Call System" for the remote reading of the tide and various elements. *The 20th Anniversary Volume of the Oceanographical Society of Japan.* (1962).

The Oceanographical Magazine
Vol. 14. No. 1, November 1962

The "Component Hour" in Darwin's Method for the Harmonic Analysis of Tides

By

Takeo Ueno

Japan Meteorological Agency

(Received November 12, 1962)

Abstract: In this paper how to get hourly tidal value in the "Component time" from hourly observation in the solar time is explained and the computed results are tabulated in the process of making "component days" in Dawin's method for the harmonic analysis of tides.

1. *Darwin's method for the harmonic analysis of tides*

It is indeed that recently more convenient and excellent methods for the tidal analysis have developed, but Darwin's method is still the most fundamental way, and the only means to get the harmonic constants available for the tidal prediction from the records with the shorter observation period than a year, which case is usual in the tidal current observations. This is also true to get only a few components such as the long period components very various compared with the other ones.

The most fundmental process in Darwin's method is to divide the hourly records into a lot of sets with the period $2\pi/n_i$ according to the component whose angle speed is n_i. The perion $2\pi/n_i$ is usually called the "component day". Superposing all the sets with the period $2\pi/n_i$, we get for the "i" component so called "the final result", from which the effects of the components with the different periods from $2\pi/ni$ vanish. As we harmonically analize the final result with 24 terms, we must divide the final result into 24 terms with the period $2\pi/24\,n_i$, which is called the "component hour". Each component hour is slight different from one solar hour, so we have to decide which of data observed every solar hour fits for which term of the final result.

2. *The case where the component hour is longer than the solar hour*

Consider M_2 component for example.

One component hour of M_2 is equal to 1.0350501 solar hours, so M component

hours corresponds to $1.035\ 0501 \times M$ solar hours.

Now we put

$$1.035\ 0501 \times M = S + x,$$

where M, S are integers, x a decimal.

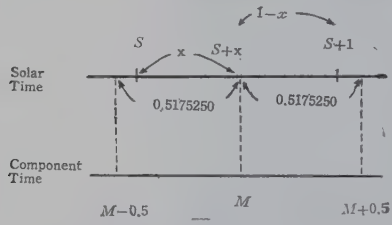

It is natural that if x is less than 1.035 0501/2, S solar hours should correspond to M component hours. Moreover such a case occurs that both x and $1-x$ are less than 1.0350501/2, where the value at the M th hour in the component time is represented by the data observed at both the S th and $(S+1)$ th solar hour. Such M hour which has two corresponding data is defined as follows:

$$0.4824750 < x < 0.5175250.$$

Those M are computed and given in the table.

3. The case where the component hour is shorter than the solar hour.

Consider K_1 component for example. One component hour of K_1 is equal to 0.9972696 solar hour, so K component hours corresponds to $0.997\ 2696 \times K$ solar hours.

Now we put

$$0.997\ 2696\ K = S + x,$$

where K, S are integers, x a decimal.

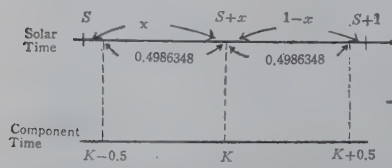

It is natural that if x is less than 0.9972696/2, S solar hours should correspond to K component hours. Moreover such a case occurs that both x and $1-x$ are more than 0.997 2696/2, where the K th hour in the component time has no corresponding solar hour. Such K hour when there is no corresponding datum is defined as follows:

$$0.4986348 < x < 0.5013652.$$

Those K are computed and given in the table.

4. The general formulas

Put n one component hour in the solar time, and

$$n \times N = S + x,$$

where N, S are integers, x a decimal.

(A) The case $n>1$.

Each N componet hour that satisfies the following condition

$$1-\frac{n}{2}<x<\frac{n}{2}$$

has two corresponding data observed every solar hour.

(B) The case $n<1$.

Each N component hour that satisfies the following condition

$$\frac{n}{2}<x<1-\frac{n}{2}$$

has no corresponding datum observed every solar hour.

The conditions for important components are as follows:

Component	n	Condition	Comment
M_2	1.035 0501	$0.482\ 4750<x<0.517\ 5250$	two corresponding data
O_1	1.075 8059	$0.462\ 0970<x<0.537\ 9030$	〃
P_1	1.002 7454	$0.498\ 6273<x<0.501\ 3727$	〃
N_2	1.054 8624	$0.472\ 5688<x<0.527\ 4312$	〃
Q_1	1.119 5149	$0.440\ 2425<x<0.559\ 7575$	〃
L_2	1.015 9684	$0.492\ 0158<x<0.507\ 9842$	〃
ν_2	1.052 1670	$0.473\ 9165<x<0.526\ 0835$	〃
μ_2	1.072 6465	$0.463\ 6768<x<0.536\ 3232$	〃
MS_4	1.017 2232	$0.491\ 3884<x<0.508\ 6116$	〃
K_1	0.997 2696	$0.498\ 6348<x<0.501\ 3652$	no corresponding datum

The computed results are given in the tables, where the first number is date, the next hour, in the component time respectively.

5. *The long period components.*

In this case the data to be analized are the daily mean sea levels which represent the value at the center of each day. Then the epoch becomes the center of the first day. In the same way as above mentioned, We can deduce the component day J which has the two corresponding solar day $(D-1)$ and D, where the following relations exist.

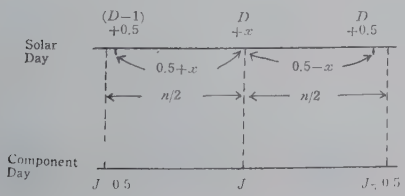

$$\begin{cases}0.5+n\times J=D+x\,,\\ 0.5-x<n/2\,,\\ 0.5+x<n/2\,.\end{cases}$$

The formula for each component is

$$0.93080 < x < 0.06920 \quad \text{for} \quad Mf,$$
$$0.925947 < x < 0.074053 \quad \text{for} \quad Mm,$$
$$0.884771 < x < 0.115239 \quad \text{for} \quad Msf.$$

For *Sa* and *Ssa*, the following method will be better. When the next relations exist

$$\begin{cases} 0.5+n(J-0.5)=D+x & 0.5<x, \\ 0.5+n(J+0.5)=D'+x' & x'<0.5, \end{cases}$$

the dates from D to D' correpond to the component day J.

Acknowledgement: The author wishes to express his sincere thanks to Dr. NAKANO who suggested me this computation ten years ago, and Prof. IMAMICHI who encouraged me to complete this paper when I was graduated from the Tokyo Science College. The writer also wishes to thank Dr. TERADA and Dr. FUTI who gave me the opportunity to publish this paper on this magazine. Mr. SHINSHI and Mr. INOUE kindly advised me to print this work and Miss AMANO typed this paper. This paper would not have published for ever without their kind assistance.

References

NAKANO, M. (1940): Choseki-gaku (The Tides) (in Japanese). Kokin-shoin, Tokyo.

Table 1. M_2. There are two observations corresponding to the dates undermentioned.

d	h	d	h	d	h	d	h	d	h	d	h	d	h	d	h	d	h	d	h	d	h
0	14	1	19	2	23	3	—	4	4	5	8	6	13	7	17	8	22	9	—	10	3	11	7
12	12	13	16	14	21	15	—	16	1	17	6	18	10	19	15	20	19	21	—	22	0	23	4
24	9	25	13	26	18	27	22	28	—	29	3	30	8	31	12	32	17	33	21	34	—	35	2
36	6	37	11	38	15	39	20	40	—	41	0	42	5	43	9	44	14	45	18	46	23	47	—
48	3	49	8	50	13	51	17	52	22	53	—	54	2	55	7	56	11	57	16	58	20	59	—
60	1	61	5	62	10	63	14	64	19	65	23	66	—	67	4	68	9	69	13	70	18	71	22
72	—	73	3	74	7	75	12	76	16	77	21	78	—	79	1	80	6	81	10	82	15	83	19
84	—	85	0	86	4	87	9	88	14	89	18	90	23	91	—	92	3	93	8	94	12	95	17
96	21	97	—	98	2	99	6	100	11	101	15	102	20	103	—	104	0	105	5	106	9	107	14
108	19	109	23	110	—	111	4	112	8	113	13	114	17	115	22	116	—	117	2	118	7	119	11
120	16	121	20	122	—	123	1	124	5	125	10	126	15	127	19	128	—	129	0	130	4	131	9
132	13	133	18	134	22	135	—	136	3	137	7	138	12	139	16	140	21	141	—	142	1	143	6
144	10	145	15	146	20	147	—	148	0	149	5	150	9	151	14	152	18	153	23	154	—	155	3
156	8	157	12	158	17	159	21	160	—	161	2	162	6	163	11	164	15	165	20	166	—	167	1
168	5	169	10	170	14	171	19	172	23	173	—	174	4	175	8	176	13	177	17	178	22	179	—

d	h	d	h	d	h	d	h	d	h	d	h	d	h	d	h	d	h	d	h	d	h
180	2	181	7	182	11	183	16	184	21	185	—	186	1	187	6	188	10	189	15	190	19	191	–
192	0	193	4	194	9	195	13	196	18	197	22	198	—	199	3	200	7	201	12	202	16	203	21
204	—	205	2	206	6	207	11	208	15	209	20	210	—	211	0	212	5	213	9	214	14	215	18
216	23	217	—	218	3	219	8	220	12	221	17	222	21	223	—	224	2	225	7	226	11	227	16
228	20	229	—	230	1	231	5	232	10	233	14	234	19	235	23	236	—	237	4	238	8	239	13
240	17	241	22	242	—	243	3	244	7	245	12	246	16	247	21	248	—	249	1	250	6	251	10
252	15	253	19	254	—	255	0	256	4	257	9	258	13	259	18	260	22	261	—	262	3	263	8
264	12	265	17	266	21	267	—	268	2	269	6	270	11	271	15	272	20	273	—	274	0	275	5
276	9	277	14	278	18	279	23	280	—	281	3	282	8	283	13	284	17	285	22	286	—	287	2
288	7	289	11	290	16	291	20	292	—	293	1	294	5	295	10	296	14	297	19	298	23	299	—
300	4	301	9	302	13	303	18	304	22	305	—	306	3	307	7	308	12	309	16	310	21	311	—
312	1	313	6	314	10	315	15	316	19	317	—	318	0	319	4	320	9	321	14	322	18	323	23
324	—	325	3	326	8	327	12	328	17	329	21	330		331	2	332	6	333	11	334	15	335	20
336	—	337	0	338	5	339	9	340	14	341	19	342	23	343	—	344	4	345	8	346	13	347	17

Table 2. P_1. There are two observations corresponding to the dates undermentioned.

d	h	d	h	d	h	d	h	d	h	d	h	d	h	d	h	d	h	d	h	d	h
7	14	22	18	37	23	53	3	68	7	83	11	98	16	113	20	129	0	144	4	159	9	174	13
189	17	204	21	220	2	235	6	250	10	265	14	280	19	295	23	311	3	326	7	341	12	356	16

Table 3. K_1. There is no observations corresponding to the dates undermentioned.

d	h	d	h	d	h	d	h	d	h	d	h	d	h	d	h	d	h	d	h	d	h
7	15	22	21	38	4	53	10	68	16	83	22	99	5	114	11	129	17	144	23	160	6	175	12
190	18	206	0	221	7	236	13	251	19	267	1	282	8	297	14	312	20	328	2	343	9	358	15

Table 4. O_1. There are two observations corresponding to the dates undermentioned.

d	h	d	h	d	h	d	h	d	h	d	h	d	h	d	h	d	h	d	h	d	h	d	h
0	7	0	20	1	9	1	22	2	11	3	1	3	14	4	3	4	16	5	5	5	19	6	8
6	21	7	10	7	23	8	12	9	2	9	15	10	4	10	17	11	6	11	20	12	9	12	22
13	11	14	0	14	14	15	3	15	16	16	5	16	18	17	8	17	21	18	10	18	23	19	12
20	1	20	15	21	4	21	17	22	6	22	19	23	9	23	22	24	11	25	0	25	13	26	3
26	16	27	5	27	18	28	7	28	21	29	10	29	23	30	12	31	1	31	15	32	4	32	17
33	6	33	19	34	8	34	22	35	11	36	0	36	13	37	2	37	16	38	5	38	18	39	7
39	20	40	10	40	23	41	12	42	1	42	14	43	4	43	17	44	6	44	19	45	8	45	21
46	11	47	0	47	13	48	2	48	15	49	5	49	18	50	7	50	20	51	9	51	23	52	12
53	1	53	14	54	3	54	17	55	6	55	19	56	8	56	21	57	11	58	0	58	13	59	2
59	15	60	4	60	18	61	7	61	20	62	9	62	22	63	12	64	1	64	14	65	3	65	16

d	h	d	h	d	h	d	h	d	h	d	h	d	h	d	h	d	h	d	h	d	h
66	6	66	18	67	8	67	21	68	10	69	0	69	13	70	2	70	15	71	4	71	18	72	7
72	20	73	9	73	22	74	11	75	1	75	14	76	3	76	16	77	5	77	19	78	8	78	21
79	10	79	23	80	12	81	2	81	15	82	4	82	17	83	7	83	20	84	9	84	22	85	11
86	0	86	14	87	3	87	16	88	5	88	18	89	8	89	21	90	10	90	23	91	12	92	2
92	15	93	4	93	17	94	6	94	20	95	9	95	22	96	11	97	0	97	14	98	3	98	16
99	5	99	18	100	7	100	21	101	10	101	23	102	12	103	1	103	15	104	4	104	17	105	6
105	19	106	9	106	22	107	11	108	0	108	13	109	3	109	16	110	5	110	18	111	7	111	20
112	10	112	23	113	12	114	1	114	14	115	4	115	17	116	6	116	19	117	8	117	22	118	11
119	0	119	13	120	2	120	16	121	5	121	18	122	7	122	20	123	10	123	23	124	12	125	1
125	14	126	3	126	17	127	6	127	19	128	8	128	21	129	11	130	0	130	13	131	2	131	15
132	5	132	18	133	7	133	20	134	9	134	23	135	12	136	1	136	14	137	3	137	16	138	6
138	19	139	8	139	21	140	10	141	0	141	13	142	2	142	15	143	4	143	18	144	7	144	20
145	9	145	22	146	12	147	1	147	14	148	3	148	16	149	6	149	19	150	8	150	21	151	10
151	23	152	13	153	2	153	15	154	4	154	17	155	7	155	20	156	9	156	22	157	11	158	1
158	14	159	3	159	16	160	5	160	19	161	8	161	21	162	10	162	23	163	12	164	2	164	15
165	4	165	17	166	6	166	20	167	9	167	21	168	11	169	0	169	14	170	3	107	16	171	5
171	18	172	8	172	21	173	10	173	23	174	12	175	2	175	15	176	4	176	17	177	6	177	19
178	9	178	22	179	11	180	0	180	13	181	3	181	16	182	5	182	18	183	7	183	21	184	10
184	23	185	12	186	1	186	15	187	4	187	17	188	6	188	19	189	9	189	22	190	11	191	0
191	13	192	2	192	16	193	5	193	18	194	7	194	20	195	10	195	23	196	12	197	1	197	14
198	4	198	17	199	6	199	19	200	8	200	22	201	11	202	0	202	13	203	2	203	15	204	5
204	18	205	7	205	20	206	9	206	23	207	12	208	1	208	14	209	3	209	17	210	6	210	19
211	8	211	21	212	11	213	0	213	13	214	2	214	15	215	5	215	18	216	7	216	20	217	9
217	22	218	12	219	1	219	14	220	3	220	16	221	6	221	19	222	8	222	21	223	10	224	0
224	13	225	2	225	15	226	4	226	18	227	7	227	20	228	9	228	22	229	11	230	1	230	14
231	3	231	16	232	5	232	19	233	8	233	21	234	10	234	23	235	13	236	2	236	15	237	4
237	17	238	7	238	20	239	9	239	22	240	11	241	1	241	14	242	3	242	16	243	5	243	18
244	8	244	21	245	10	245	23	246	12	247	2	247	15	248	4	248	17	249	6	249	20	250	9
250	22	251	11	252	0	252	14	253	3	253	16	254	5	254	18	255	7	255	21	256	10	256	23
257	12	258	1	258	15	259	4	259	17	260	6	260	19	261	9	261	22	262	11	263	0	263	13
264	3	264	16	265	5	265	18	266	7	266	21	267	10	267	23	268	12	269	1	269	14	270	4
270	17	271	6	271	19	272	8	272	22	273	11	274	0	274	13	275	2	275	16	276	5	276	18
277	7	277	20	278	10	278	23	279	12	280	1	280	14	281	3	281	17	282	6	282	19	283	8
283	21	284	11	285	0	285	13	286	2	286	15	287	5	287	18	288	7	288	20	289	9	289	23
290	12	291	1	291	14	292	3	292	17	293	6	293	19	294	8	294	21	295	10	296	0	296	13
297	2	297	15	298	4	298	18	299	7	299	20	300	9	300	22	301	12	302	1	302	14	303	3
303	16	304	6	304	19	305	8	305	21	306	10	307	0	307	13	308	2	308	15	309	4	309	17
310	7	310	20	311	9	311	22	312	11	313	1	313	14	314	3	314	16	315	5	315	19	316	8
316	21	317	10	317	23	318	13	319	2	319	15	320	4	320	17	321	6	321	20	322	9	322	22
323	11	324	0	324	14	325	3	325	16	326	5	326	18	327	8	327	21	328	10	328	23	329	12
330	2	330	15	331	4	331	17	332	6	332	20	333	9	333	22	334	11	335	0	335	3	336	3
336	16	337	5	337	18	338	7	338	21	339	10	339	23	340	12	341	1	341	15	342	4	342	17
343	6	343	19	344	9	344	12	345	11	346	0	346	13	347	2	347	16	348	5	348	18	349	7
349	20	350	10																				

Table 5. N_2 There are two observations corresponding to the dates undermentioned.

d	h	d	h	d	h	d	h	d	h	d	h	d	h	d	h	d	h	d	h	d	h	d	h
0	9	1	3	1	22	2	16	3	10	4	4	4	22	5	17	6	11	7	5	7	23	8	18
9	12	10	6	11	0	11	19	12	13	13	7	14	1	14	19	15	14	16	8	17	2	17	20
18	15	19	9	20	3	20	21	21	15	22	10	23	4	23	22	24	16	25	11	26	5	26	23
27	17	28	12	29	6	30	0	30	18	31	12	32	7	33	1	33	19	34	13	35	8	36	2
36	20	37	14	38	8	39	3	39	19	40	15	41	9	42	4	42	22	43	16	44	10	45	5
45	23	46	17	47	11	48	5	49	0	49	18	50	12	51	6	52	1	52	19	53	13	54	7
55	1	55	20	56	14	57	8	58	2	58	21	59	15	60	9	61	3	61	22	62	16	63	10
64	4	64	22	65	17	66	11	67	5	67	23	68	18	69	12	70	6	71	0	71	18	72	13
73	7	74	1	74	19	75	14	76	8	77	2	77	20	78	15	79	9	80	3	80	21	81	15
82	10	83	4	83	22	84	16	85	11	86	5	86	23	87	17	88	11	89	6	90	0	90	18
91	12	92	7	93	1	93	19	94	13	95	8	96	2	96	20	97	14	98	8	99	3	99	21
100	15	101	9	102	4	102	22	103	16	104	10	105	4	105	23	106	17	107	11	108	5	109	0
109	18	110	12	111	6	112	1	112	19	113	13	114	7	115	1	115	20	116	14	117	8	118	2
118	21	119	15	120	9	121	3	121	22	122	16	123	10	124	44	124	22	125	17	126	11	127	5
127	23	128	18	129	12	130	6	131	0	131	18	132	13	133	7	134	1	134	19	135	14	136	8
137	2	137	20	138	15	139	9	140	3	140	21	141	15	142	10	143	4	143	22	144	16	145	11
146	5	146	23	147	17	148	11	149	6	150	0	150	18	151	12	152	7	153	1	153	19	154	13
155	8	156	2	156	20	157	14	158	8	159	3	159	21	160	15	161	9	162	4	162	21	163	16
164	10	165	4	165	23	166	17	167	11	168	5	169	0	169	18	170	12	171	6	172	1	172	19
173	13	174	7	175	1	175	20	176	14	177	8	178	2	178	21	179	5	180	9	181	3	181	21
182	16	183	10	184	4	184	22	185	17	186	11	187	5	187	23	188	18	189	12	190	6	191	0
191	18	192	13	193	7	194	1	194	19	195	14	196	8	197	2	197	20	198	14	199	9	200	3
200	21	201	15	202	10	203	4	203	22	204	16	205	11	206	5	206	23	207	17	208	11	209	6
210	0	210	18	211	12	212	7	213	1	213	19	214	13	215	7	216	2	216	20	217	14	218	8
219	3	219	21	220	15	221	9	222	4	222	22	223	16	224	10	225	4	225	23	226	17	227	11
228	5	229	0	229	18	230	12	231	6	232	0	232	19	233	13	234	7	235	1	235	20	236	14
237	8	238	2	238	21	239	15	240	9	241	3	241	21	242	16	243	10	244	4	244	22	245	17
246	11	247	5	247	23	248	17	249	12	250	6	251	0	251	18	252	13	253	7	254	1	254	19
255	14	256	8	257	2	257	20	258	14	259	9	260	3	260	21	261	15	262	10	263	4	263	22
264	16	265	10	266	5	266	23	267	17	268	11	269	6	270	0	270	18	271	12	272	7	273	1
273	19	274	13	275	7	276	2	276	20	277	14	278	8	279	3	279	21	280	15	281	9	282	3
282	22	283	16	284	10	285	4	285	23	286	17	287	11	288	5	289	0	289	18	290	12	291	6
292	0	292	19	293	13	294	7	295	1	295	20	296	14	297	8	298	2	298	20	299	15	300	9
301	3	301	21	302	16	303	10	304	4	304	22	305	17	306	11	307	5	307	23	308	17	309	12
310	6	311	0	311	18	312	13	313	7	314	1	314	19	315	13	316	8	317	2	317	20	318	14
319	9	320	3	320	21	321	15	322	10	323	4	323	22	324	16	325	10	326	5	326	23	327	17
328	11	329	6	330	0	330	18	331	12	332	6	333	1	333	19	334	13	335	7	336	2	336	20
337	14	338	8	339	3	339	21	340	15	341	9	342	3	342	22	343	16	344	10	345	4	345	23
346	17	347	11	348	5	348	23	349	18	350	12	351	6	352	0	352	19	353	13	354	7	355	1
355	20	356	14	357	8	358	2	358	20	359	15	360	9	361	3	361	21	362	16	363	10	364	4
364	22	365	17	366	11	367	5	367	23	368	17	369	12										

Table 6. Q_1. There are two observations corresponding to the dates undermentioned.

d	h	d	h	d	h	d	h	d	h	d	h	d	h	d	h	d	h	d	h	d	h	d	h
0	4	0	13	0	21	1	5	1	14	1	22	2	6	2	15	2	23	3	7	3	16	4	0
4	9	4	17	5	1	5	10	5	18	6	2	6	11	6	19	7	4	7	12	7	20	8	5
8	13	8	21	9	6	9	14	9	22	10	7	10	15	11	0	11	8	11	16	12	1	12	9
12	17	13	2	13	10	13	19	14	3	14	11	14	20	15	4	15	12	15	21	16	5	16	13
16	22	17	6	17	15	17	23	18	7	18	16	19	0	19	8	19	17	20	1	20	9	20	18
21	2	21	11	21	19	22	3	22	12	22	20	23	4	23	13	23	21	24	6	24	14	24	22
25	7	25	15	25	23	26	8	26	16	27	0	29	9	27	17	28	2	28	10	28	18	29	3
29	11	29	19	30	4	30	12	30	20	31	5	31	13	31	22	32	6	32	14	32	23	33	7
33	15	34	0	34	8	34	17	35	1	35	9	35	18	36	2	36	10	36	19	37	3	37	11
37	20	38	4	38	13	38	21	39	5	39	14	39	22	40	6	40	15	40	23	41	8	41	16
42	0	42	9	42	17	43	1	43	10	43	18	44	2	44	11	44	19	45	4	45	12	45	20
46	5	46	13	46	21	47	6	47	14	47	22	48	7	48	15	49	0	49	8	49	16	50	1
50	9	50	17	51	2	51	10	51	19	52	3	52	11	52	20	53	4	53	12	53	21	54	5
54	13	54	22	55	6	55	15	55	23	56	7	56	16	57	0	57	8	57	17	58	1	58	9
58	18	59	2	59	11	59	19	60	3	60	12	60	20	61	4	61	13	61	21	62	6	62	14
62	22	63	7	63	15	63	23	64	8	64	16	65	0	65	9	65	17	66	2	66	10	66	18
67	3	67	11	67	19	68	4	68	12	68	21	69	5	69	13	69	22	70	6	70	14	70	23
71	7	71	15	72	0	72	8	72	17	73	1	73	9	73	18	74	2	74	10	74	19	75	3
75	11	75	20	76	4	76	13	76	21	77	5	77	14	77	22	78	6	78	15	78	23	79	8
79	16	80	0	80	9	80	17	81	1	81	10	81	18	82	2	82	11	82	19	83	4	83	12
83	20	84	5	84	13	84	21	85	6	85	14	85	23	86	7	86	15	87	0	87	8	87	16
88	1	88	9	88	17	89	2	89	10	89	19	90	3	90	11	90	20	91	4	91	12	91	21
92	5	92	13	92	22	93	6	93	15	93	23	94	7	94	16	95	0	95	8	95	17	96	1
96	10	96	18	97	2	97	11	97	19	98	3	98	12	98	20	99	4	99	13	99	21	100	6
100	14	100	22	101	7	101	15	101	23	102	8	102	16	130	0	103	9	103	17	104	2	104	10
104	18	105	3	105	11	105	19	106	4	106	12	106	21	107	5	107	13	107	22	108	6	108	14
108	23	109	7	109	15	110	0	110	8	110	17	111	1	111	9	111	18	111	2	112	10	112	19
113	3	113	12	113	20	114	4	114	13	114	21	115	5	115	14	115	22	116	6	116	15	116	23
117	8	117	16	118	0	118	9	118	17	119	1	119	10	119	18	120	2	120	11	120	19	121	4
121	12	121	20	122	5	122	13	122	21	123	6	123	14	123	23	124	7	124	15	125	0	125	8
125	16	126	1	126	9	126	17	127	2	127	10	127	19	128	3	128	11	128	20	129	4	129	12
129	21	130	5	130	14	130	22	131	6	131	15	131	23	132	7	132	16	133	0	133	8	133	17
134	1	134	10	134	18	135	2	135	11	135	19	136	3	136	12	136	20	137	4	137	13	137	21
138	6	138	14	138	22	139	7	139	15	139	23	140	8	140	16	141	1	141	9	141	17	142	2
142	10	142	18	143	3	143	11	143	19	144	4	144	12	144	21	145	5	145	13	145	22	146	6
146	14	146	23	147	7	147	15	148	0	148	8	148	17	149	1	149	9	149	18	150	2	150	10
150	19	151	3	151	12	151	20	152	4	152	13	152	21	153	5	153	14	153	22	154	6	154	15
154	23	155	8	155	16	156	0	156	9	156	17	157	1	157	10	157	18	158	3	158	11	158	19
159	4	159	12	159	20	160	5	106	13	160	21	161	6	161	14	161	23	162	7	162	15	163	0
163	8	163	16	164	1	164	9	164	17	165	2	165	10	165	19	166	3	166	11	166	20	167	4
167	12	167	21	168	5	168	14	168	22	169	6	169	15	169	23	170	7	170	16	171	0	171	8
171	17	172	1	172	10	172	18	173	2	173	11	173	19	174	3	174	12	174	20	175	4	175	13
175	21	176	6	176	14	176	22	177	7	177	15	177	23	178	8	178	16	179	1	179	9	179	17
180	2	180	10	180	18	181	3	181	11	181	19	182	4	182	12	182	21	183	5	183	13	183	22
184	6	184	14	184	23	185	7	185	16	186	0	186	8	186	17	187	1	187	9	187	18	188	2
188	10	188	19	189	3	189	12	189	20	190	4	190	13	190	21	191	5	191	14	191	22	192	6
192	15	192	23	193	8	193	16	194	0	194	9	194	17	195	1	195	10	195	18	196	3	196	11
196	19	197	4	197	12	197	20	198	5	198	13	198	21	199	6	199	14	199	23	200	7	200	15

d	h	d	h	d	h	d	h	d	h	d	h	d	h	d	h	d	h	d	h	d	h	d	h
201	0	201	8	201	16	202	1	202	9	202	18	203	2	203	10	203	19	204	3	204	11	204	20
205	4	205	12	205	21	206	5	206	14	206	22	207	6	207	15	207	23	208	7	208	16	209	0
209	8	209	17	210	1	210	10	210	18	211	2	211	11	211	19	212	3	212	12	212	20	213	5
213	13	213	21	214	6	214	14	214	22	215	7	215	15	215	23	216	8	216	16	217	1	217	9
217	17	218	2	218	10	218	18	219	3	219	11	219	19	220	4	220	12	220	21	221	5	221	13
221	22	222	6	222	14	222	23	223	7	223	16	224	0	224	8	224	17	225	1	225	9	225	18
226	2	226	10	226	19	227	3	227	12	227	20	228	4	228	13	228	21	229	5	229	14	229	22
230	7	230	15	230	23	231	8	231	16	232	0	232	9	232	17	233	1	233	10	233	18	234	3
234	11	234	19	235	4	235	12	235	20	236	5	236	13	236	21	237	6	237	14	237	23	238	7
238	15	239	0	239	8	239	16	240	1	240	9	240	18	241	2	241	10	241	19	242	3	242	11
242	20	243	4	243	12	243	21	244	5	244	14	244	22	245	6	245	15	245	23	246	7	246	16
247	0	247	8	247	17	248	1	248	10	248	18	249	2	249	11	249	19	250	3	250	12	250	20
251	5	251	13	251	21	252	6	252	14	252	22	253	7	253	15	253	23	254	8	254	16	255	1
255	9	255	17	256	2	256	10	256	18	257	3	257	11	257	20	258	4	258	12	258	21	259	5
259	13	259	22	260	6	260	14	260	23	261	7	261	16	262	0	262	8	262	17	263	1	263	9
263	18	264	2	264	10	264	19	265	3	265	12	265	20	266	4	266	13	266	21	267	5	267	14
267	22	268	7	268	15	268	23	269	8	269	16	270	0	270	9	270	17	271	1	271	10	271	18
272	3	272	11	272	19	273	4	273	12	273	20	274	5	274	13	274	22	275	6	275	14	275	23
276	7	276	15	277	0	277	8	277	16	278	1	278	9	278	18	279	2	279	10	279	19	280	3
280	11	280	20	281	4	281	12	281	21	282	5	282	14	282	22	283	6	283	15	283	23	284	7
284	16	285	0	285	9	285	17	286	1	286	10	286	18	287	2	287	11	287	19	288	3	288	12
288	20	289	5	289	13	299	21	290	6	290	14	290	22	291	7	291	15	291	23	292	8	292	16
293	1	293	9	293	17	294	2	294	10	294	18	295	3	295	11	295	20	296	4	296	12	296	21
297	5	297	13	298	22	298	6	298	14	298	23	299	7	299	16	200	0	200	8	300	17	301	1
301	9	301	18	302	2	302	11	302	19	303	3	303	12	303	20	304	4	304	13	304	21	305	5
305	14	305	22	206	7	306	15	306	23	307	8	307	16	308	0	308	9	308	17	309	1	309	10
309	18	310	3	310	11	310	19	311	4	311	12	311	20	312	5	312	13	312	22	313	6	313	14

Table 7. L_2. There are two observations corresponding to the dates undermentioned.

d	h	d	h	d	h	d	h	d	h	d	h	d	h	d	h	d	h	d	h	d	h	d	h
1	7	3	22	6	13	9	3	11	18	14	8	16	23	19	14	22	4	24	19	27	10	30	0
32	15	35	5	37	20	40	11	43	1	45	16	48	7	50	21	53	12	56	2	58	17	61	8
63	22	66	13	69	4	71	18	74	9	56	23	79	14	82	5	84	19	87	10	90	0	92	15
95	6	97	20	100	11	103	2	105	16	108	7	110	22	113	12	116	3	118	17	121	8	123	23
126	13	129	4	131	18	134	9	137	0	139	14	142	5	144	20	147	10	150	1	152	15	155	6
157	21	160	11	163	2	165	17	168	7	170	22	173	12	176	3	178	18	181	8	183	23	186	14
189	4	191	19	194	9	197	0	199	15	202	5	204	20	207	11	210	1	212	16	215	6	217	21
220	12	223	2	225	17	228	8	230	22	233	13	236	3	238	18	241	9	243	23	246	14	249	5
251	19	254	10	257	0	259	15	262	6	264	20	267	11	270	2	272	16	275	7	277	21	280	12
283	3	285	17	288	8	290	23	293	13	296	4	298	18	301	9	304	0	306	14	209	5	311	20
314	10	317	1	319	15	322	6	324	21	327	11	330	2	332	17	335	7	337	22	340	12	343	3
345	18	348	8	350	23	353	14	356	4	358	19	361	9	364	0	366	15	369	5				

Table 8. MS_4. There are two observations corresponding to the dates undermentioned.

d	h	d	h	d	h	d	h	d	h	d	h	d	h	d	h	d	h	d	h	d	h	d	h
1	5	3	15	6	1	8	11	10	21	13	7	15	17	18	3	20	14	23	0	25	10	27	20
30	6	32	16	35	2	37	12	39	22	42	8	44	18	47	4	49	14	52	0	54	10	56	20
59	6	61	17	64	3	66	13	68	23	71	9	73	19	76	5	78	15	81	1	83	11	85	21
88	7	90	17	93	3	95	13	97	23	100	10	102	20	105	6	107	16	110	2	112	12	114	22
117	8	119	18	122	4	124	14	127	0	129	10	131	20	134	6	136	16	139	3	141	13	143	23
146	9	148	19	151	5	153	15	156	1	158	11	160	21	163	7	165	17	168	3	170	13	172	23
175	9	177	19	180	6	182	16	185	2	188	12	189	22	192	8	194	18	197	4	199	14	202	0
204	10	206	20	209	6	211	16	214	2	216	12	218	23	221	9	223	19	226	5	228	15	231	1
233	11	235	21	238	7	240	17	243	3	245	13	247	23	250	9	252	19	255	5	257	16	260	2
262	12	264	22	267	8	269	18	272	4	274	14	277	0	279	10	281	20	284	6	286	16	289	2
291	12	293	22	296	8	298	19	301	5	303	15	306	1	308	11	310	21	313	7	315	17	318	3
320	13	322	23	325	9	327	19	330	5	332	15	335	1	337	12	339	22	342	8	344	18	347	4
349	14	352	0	354	10	356	20	359	6	361	16	364	2	366	12	368	22						

昭和38年1月21日印刷
昭和38年1月25日発行

編集兼発行人　気象庁
東京都千代田区大手町一ノ七

印刷者　花崎実
東京都中央区新富町二ノ十九

印刷所　大東印刷工芸株式会社
東京都中央区新富町二ノ十九